Restriction of C1-inhibitor activity in hereditary angioedema by dominant-negative effects of disease-associated *SERPING1* gene variants

Laura Barrett Ryø, MSc,[a] Didde Haslund, PhD,[a] Anne Bruun Rovsing, PhD,[a] Rasmus Pihl, PhD,[a] Wariya Sanrattana, PhD,[b] Steven de Maat, PhD,[b] Yaseelan Palarasah, PhD,[c,d] Coen Maas, PhD,[b,e] Steffen Thiel, PhD,[a] and Jacob Giehm Mikkelsen, PhD[a] *Aarhus, Odense, and Esbjerg, Denmark; and Utrecht, The Netherlands*

GRAPHICAL ABSTRACT

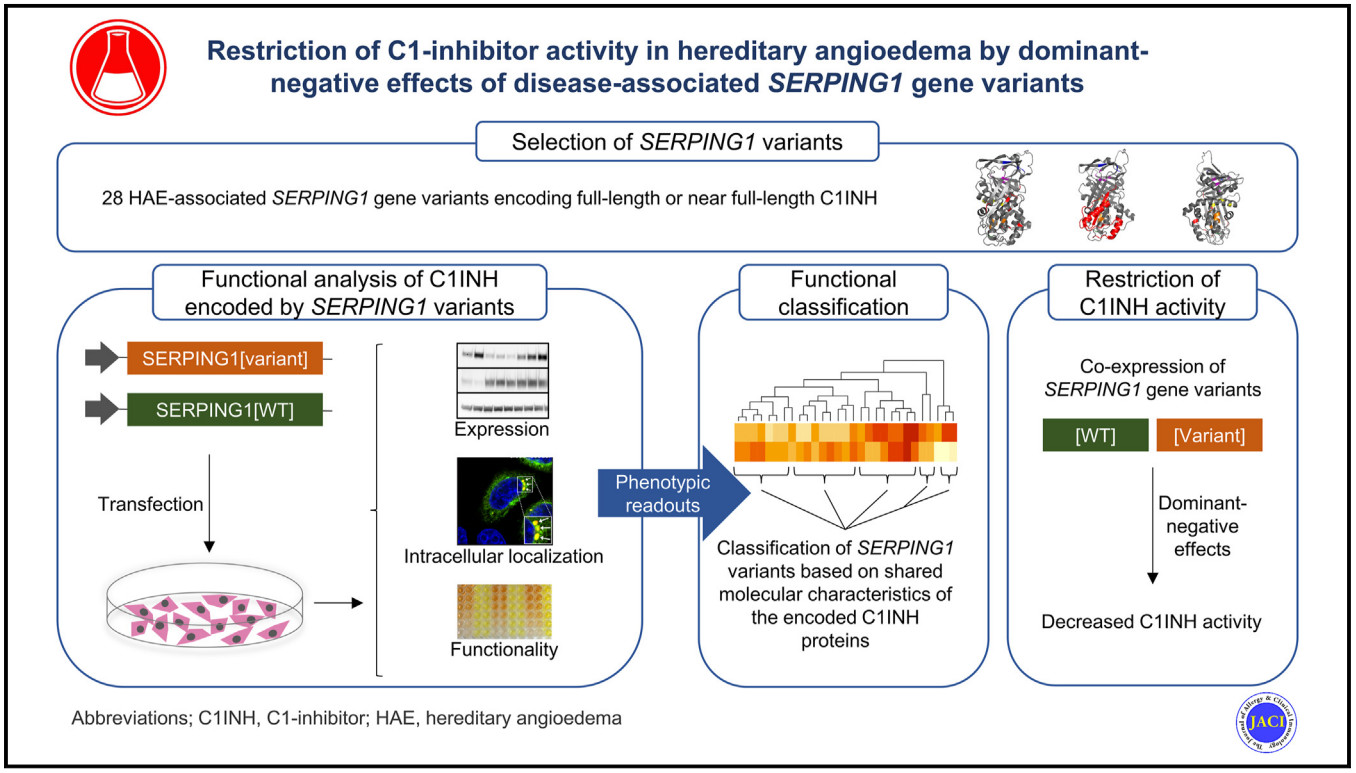

Background: Patients with hereditary angioedema experience recurrent, sometimes life-threatening, attacks of edema. It is a rare genetic disorder characterized by genetic and clinical heterogenicity. Most cases are caused by genetic variants in the *SERPING1* gene leading to plasma deficiency of the encoded protein C1 inhibitor (C1INH). More than 500 different hereditary angioedema–causing variants have been identified in the *SERPING1* gene, but the disease mechanisms by which they result in pathologically low C1INH plasma levels remain largely unknown.

Objectives: The aim was to describe *trans*-inhibitory effects of full-length or near full-length C1INH encoded by 28 disease-associated *SERPING1* variants.

Methods: HeLa cells were transfected with expression constructs encoding the studied *SERPING1* variants. Extensive and comparative studies of C1INH expression, secretion, functionality, and intracellular localization were carried out.

Results: Our findings characterized functional properties of a subset of *SERPING1* variants allowing the examined variants to be subdivided into 5 different clusters, each containing variants sharing specific molecular characteristics. For all variants except 2, we found that coexpression of mutant and normal C1INH negatively affected the overall capacity to target proteases. Strikingly, for a subset of variants, intracellular formation of C1INH foci was detectable only in heterozygous

From [a]the Department of Biomedicine, Aarhus University, Aarhus; [b]CDL Research, University Medical Center Utrecht, Utrecht University, Utrecht; [c]the Department of Cancer and Inflammation Research, University of Southern Denmark, Odense; [d]the Department of Clinical Biochemistry, Hospital of South West Jutland, Esbjerg; and [e]the Unit for Thrombosis Research, Department of Regional Health Research, University of Southern Denmark, Esbjerg.

Received for publication January 10, 2023; revised April 17, 2023; accepted for publication April 25, 2023.

Corresponding author: Jacob Giehm Mikkelsen, PhD, Department of Biomedicine, Aarhus University, Høegh-Guldbergs Gade 10, DK-8000 Aarhus C, Denmark. E-mail: giehm@biomed.au.dk.

0091-6749

https://doi.org/10.1016/j.jaci.2023.04.023

configurations enabling simultaneous expression of normal and mutant C1INH.
Conclusions: We provide a functional classification of *SERPING1* gene variants suggesting that different *SERPING1* variants drive the pathogenicity through different and in some cases overlapping molecular disease mechanisms. For a subset of gene variants, our data define some types of hereditary angioedema with C1INH deficiency as serpinopathies driven by dominant-negative disease mechanisms. (J Allergy Clin Immunol 2023;■■■:■■■-■■■.)

Key words: *Hereditary angioedema,* SERPING1*, C1 inhibitor, disease mechanism, dominant-negative, plasma kallikrein, genetics, functional classification, contact pathway*

Abbreviations used
A1AT: α_1 Antitrypsin
A1ATD: A1AT deficiency
BSA: Bovine serum albumin
C1INH: C1 inhibitor
ER: Endoplasmic reticulum
FENIB: Familial encephalopathy with neuroserpin inclusion bodies
FXIIa: Factor XIIa
HAE: Hereditary angioedema
HeLa: Human cervix epithelioid carcinoma cells
HPR: Horseradish peroxidase
MASP-1: Mannan-binding lectin serine protease 1
NO: Nitric oxide
NPT II: Neomycin phosphotransferase
PBS: Phosphate-buffered saline
pKa: Plasma kallikrein
RCL: Reactive center loop
Serpin: Serine protease inhibitor
SERPING1: Serpin family G member 1
TBS: Tris-buffered saline
WT: Wild type

Hereditary angioedema (HAE) is a rare genetic disorder characterized by recurrent episodes of edema arising in the deep dermis, submucosa, and subcutaneous tissues. The edema attacks are often localized to the extremities, the gastrointestinal tract, and the face. Still, a large proportion of the patients also experience one or several potentially fatal attacks in the upper airways.[1-3] The disorder has a substantial negative impact on the patient's quality of life and further forces a physical and emotional burden on family members. HAE is characterized by clinical and genetic heterogenicity. On the basis of the level and activity of the serine protease inhibitor (serpin) C1 inhibitor (C1INH) found in the plasma of patients, HAE is divided into 2 major types: C1INH-HAE and nC1INH-HAE. C1INH-HAE is caused by C1INH deficiency in the blood, whereas patients with nC1INH-HAE have other genetic defects and have normal levels of functional C1INH. C1INH-HAE accounts for the majority of HAE cases and predominantly follows an autosomal dominant pattern of inheritance with incomplete penetrance, whereas only a few cases of recessive inheritance have been reported.[4,5]

C1INH-HAE is caused by genetic variants in the serpin family G member 1 *(SERPING1)* gene encoding the C1INH protein,[6] leading to either quantitative or qualitative C1INH plasma deficiency.[7,8] C1INH is a serpin primarily produced in the liver, from where it is secreted into the plasma supporting a blood concentration ranging from 0.20 to 0.32 g/L.[9] Here, C1INH is a key regulator of several vital proteolytic cascades related to the complement system, the fibrinolytic system, and the contact pathway. HAE edema attacks arise as a result of poorly controlled activation of the contact pathway.[10,11] At normal plasma levels, C1INH is responsible for regulating the contact pathway by inhibiting the activity of 2 serine proteases, factor XIIa (FXIIa) and plasma kallikrein (pKa).[12,13] However, the reduced C1INH plasma levels of C1INH-HAE patients are not sufficient to uphold the necessary regulation, which leads to reduced control of activation of the contact pathway, ultimately resulting in excess release of the vasoactive peptide bradykinin from high-molecular-weight kininogen. Bradykinin binds to the G protein–coupled bradykinin B2 receptor located on the surface of endothelial cells. Downstream signaling from the B2 receptor results in increased vascular permeability through disruption of vascular endothelial cadherin and vasodilation by stimulation of the production of nitric oxide (NO).[14-19] The disruption of vascular endothelial cadherin–dependent cell–cell contacts between endothelial cells combined with NO-mediated relaxation of the vascular smooth muscle cells results in the movement of fluid from the vascular space into the interstitial compartment, resulting in edema attacks.[20-22]

Whereas the biochemical and physiological consequences of C1INH deficiency in C1INH-HAE are fairly well understood, the molecular mechanisms leading to reduced C1INH levels in C1INH-HAE patients remain largely unknown. Most patients with C1INH-HAE are heterozygous carriers of a HAE-causing *SERPING1* allele and thus carry a single wild type (WT) *SERPING1* allele. However, these patients typically present with C1INH plasma levels in the range of 5-30% compared to healthy individuals,[23-25] which is substantially lower than the 50% that would be expected from expression via a single functional allele.

On the basis of clinical observations, a C1INH plasma level corresponding to approximately 40% is considered sufficient to uphold normal C1INH function.[26] Although the pathophysiologic cause of this reduction in C1INH plasma levels remains vaguely understood, the designation *trans*-inhibition is often used to describe this phenomenon. This term alludes to molecular scenarios by which the gene products encoded by disease-causing *SERPING1* gene variants are likely to have a negative impact on any of synthesis, intracellular trafficking, or secretion of C1INH encoded by the WT *SERPING1* allele.[27-30]

More than 500 different *SERPING1* variants have been reported to cause C1INH-HAE,[31] which emphasizes C1INH-HAE's genetic heterogeneity. The wide-ranging spectrum of disease-causing *SERPING1* variants includes everything from missense mutations, nonsense mutations, splice site mutations, smaller insertions, and deletions to larger genomic deletions caused by recombination between Alu repeats. The disease-causing variants do not localize to isolated structural or functional domains but rather seem to be scattered throughout the entire gene, affecting amino acids at various locations in the tertiary structure of the protein. Consequently, transcripts from the disease-causing *SERPING1* variants are expected to encode an extensive range of C1INH proteins with potentially distinct functional defects, although in some cases, disease alleles may

not express a C1INH protein because of a premature stop codon and potential mRNA degradation due to nonsense-mediated decay.

Unlike the majority of proteins, most serpins, including C1INH, do not initially fold to their most thermodynamically stable form but are secreted in a metastable conformation.[32] Proteins of the serpin superfamily share a highly conserved tertiary structure with a core consisting of 3 beta sheets (designated sA, sB, and sC) and 8 to 9 alpha helices (designated hA-hI). Target proteases cleave C1INH within a stretch of solvent-exposed amino acids termed the reactive center loop (RCL). The metastable conformation, which is caused by the protruding structure of the RCL, is a major driving force for the mechanism by which serpins inhibit their target proteases.[33-35] The structure of the RCL matches the shape of the active site of the target serine proteases and includes a scissile bond mimicking the natural substrate for the target proteases.[36-38] Cleavage of the scissile bond triggers a conformational change in C1INH, much like the snapping of a mousetrap. The RCL inserts into sA, and the now covalently linked target protease is translocated to the opposite pole of the serpin, resulting in the serpin transitioning from a metastable to a highly stable conformation.[37,39]

Several different domains in the inhibitory serpin are crucial for the function of the kinetic trap. The primary structure of the RCL is essential for target protease specificity, whereas the length of the RCL is pivotal for the kinetic stability of the serpin–target protease complex. The hinge, an alanine-rich region of the RCL, is crucial for RCL mobility and insertion into sA.[33,40-44] The shutter and breach regions located in sA facilitate the opening of sA and initial insertion of the serpin RCL and are thus important for the appropriate conformational change resulting in the mousetrap-like snapping of the serpin.[42,45-47]

The broad spectrum of disease-causing variants and the high variability in the clinical manifestation observed among C1INH-HAE patients could indicate that different molecular disease mechanisms, all giving rise to pathogenically low levels of plasma C1INH, drive the development of the disease in unrelated patients. We have previously shown that C1INH encoded by a small subset of *SERPING1* variants impairs the secretion of normal C1INH in a dominant-negative fashion by inducing C1INH protein aggregation within the endoplasmic reticulum (ER).[48] In particular, we described that coexpression of mutated and normal C1INH resulted in a substantial reduction in the secretion of normal C1INH caused by direct protein–protein interactions between normal and mutated C1INH inside the ER. For one of the studied *SERPING1* variants causing a particularly distinct cellular phenotype, we were able to retrieve patient-derived fibroblasts and confirm the presence of C1INH aggregation inside the ER. More recently, Yasuno and colleagues[49] reported another dominant-negative *SERPING1* variant leading to retention and degradation of normal C1INH protein in the cytoplasm. By functional assessment of a subset of disease-causing *SERPING1* variants, a recent study by Ren et al[50] provided further insight into the pathogenesis of HAE; the authors identified HAE-causing *SERPING1* variants encoding C1INH protein with glycosylation abnormalities and a variant resulting in the formation of extracellular C1INH oligomers. C1INH polymers have been detected in plasma samples from C1INH-HAE patients,[51] and such C1INH polymers have been shown to activate the contact pathway *in vitro*.[52] However, their significance in relation to the molecular disease mechanisms in C1INH-HAE remains unclear. In addition, haploinsufficiency and increased C1INH metabolism have been proposed as underlying disease mechanisms in C1INH-HAE patients carrying other *SERPING1* variants, including truncated variants, which are less likely to interfere with the secretion of normal C1INH protein.[53-55]

In the present study, we further elucidate the complexity of the underlying molecular disease mechanisms in C1INH-HAE. On the basis of extensive molecular studies of what is to our knowledge the largest ever studied panel of selected *SERPING1* variants, we explore patterns of expression, intracellular localization, and functionality of the encoded C1INH proteins, alone and coexpressed with normal C1INH to mimic a heterozygous state. This allows us to subdivide the studied *SERPING1* variants into 5 different clusters, each sharing distinct molecular characteristics. Furthermore, we find that coexpression together with the WT *SERPING1* allele of all but 2 of the studied *SERPING1* variants has negative impact on the overall capacity to inhibit proteases in the supernatant from cotransfected cells. Collectively, our data suggest that some types of HAE-causing *SERPING1* variants coexisting with WT *SERPING1* alleles result in reduced overall C1INH activity by *trans*-acting negative effects elicited through molecular mechanisms acting with different weight depending on the disease-causing gene variant.

METHODS

Vector construction

The expression plasmids were generated as described in Haslund et al.[48] The expression plasmid encoding the ER-resident calreticulin-Tomato fusion protein, the tdTomato–ER-3 vector, was a gift from Matteo Beretta, King's College London (Addgene 58097).

Cell culture

Human cervix epithelioid carcinoma cells (HeLa) used to conduct experiments presented in all figures, as well as in supplementary figures in this article's Online Repository available at www.jacionline.org, were acquired through ATCC and maintained in Dulbecco modified Eagle medium (Lonza) supplemented with 5% fetal calf serum, 100 U/mL penicillin, and 100 μg/mL streptomycin and cultured at 37°C in 5% (v/v) CO_2.

Western blot analysis

For all Western blots, transfected cells were lysed on ice using RIPA Lysis and Extraction buffer (Thermo Fisher Scientific, 89901) supplemented with 10 mmol NaF and 1× complete protease inhibitor cocktail (Roche, 5892970001). XT Sample buffer, 4X (Bio-Rad, 161-0791) and XT Reducing Agent, 20× (Bio-Rad, 161-0792), were added to the samples before 5 minutes' incubation at 95°C. Proteins were separated by sodium dodecyl sulfate–polyacrylamide gel electrophoresis on a 4-15% gel (Bio-Rad, 5671084) and blotted onto a polyvinylidene fluoride membrane (Bio-Rad, 1704157). Membranes were blocked in 5% skim milk (Tris-buffered saline [TBS], 0.005% Tween 20) at room temperature for 1 hour on a rocking table and then incubated with the primary antibody (TBS + 0.005% Tween 20 + 2.5% bovine serum albumin [BSA]) on a rocking table at 4°C

overnight. Membranes were then washed (TBS + 0.005% Tween 20) and incubated with a horseradish peroxidase (HPR)-conjugated secondary antibody (1× TBS + 0.005% Tween 20 + 2.5% BSA) for 1 hour at room temperature on a tilt. After incubation with the secondary antibody, the membranes were washed (TBS + 0.005% Tween 20 + 2.5% BSA) and visualized with chemiluminescence using a horseradish peroxidase substrate (Bio-Rad, 170-5061). If more than 1 protein was to be visualized on the membranes, the membranes were either cut into different sections and the proteins visualized as described above, or the membranes were washed (TBS + 0.005% Tween 20), stripped using Restore PLUS Western Blot Stripping Buffer (Thermo Fisher Scientific, 46430), washed (TBS + 0.005% Tween 20), blocked in 5% skim milk (TBS + 0.005% Tween 20), and visualized as described above. The light emission from the blots were recorded on an ImageQuant LAS 4000 mini device. The signals (ie, the band volumes) of individual bands were analyzed by ImageJ software (imagej.nih.gov/ij).

Separation of soluble and insoluble fractions

Separation of soluble and insoluble fractions of cell lysates was carried out as described in Haslund et al.[48] Briefly, HeLa cells were seeded in 6-well plates at a density of 2×10^5 cells per well on day 1. At 24 hours after seeding, the cells were transfected with a total amount of 900 ng pDNA using Turbofect (Thermo Fisher Scientific). For analysis of separately expressed *SERPING1* variants, HeLa cells were transfected with 900 ng pSERPING1[variant]. For the coexpression studies, HeLa cells were transfected with 450 ng pSERPING1[WT]-V5 and 450 ng pSERPING1[variant]. At 24 hours after transfection, the medium was replaced with 1.5 mL fresh medium. The cells were collected 72 hours after transfection. The cell pellets were washed 3 times in phosphate-buffered saline (PBS) and thereafter lysed on ice using RIPA Lysis and Extraction buffer (Thermo Fisher Scientific, 89901) supplemented with 10 mmol NaF and 1× complete protease inhibitor cocktail (Roche, 5892970001). Cell lysates were centrifuged at 13,000 × *g* for 30 minutes at 4°C, and the supernatant constituting the soluble fraction was moved to a new tube. The remaining pellet comprising the insoluble fraction was washed 3 times in PBS to avoid carryover from the soluble fraction and then resuspended in 100 μL buffer containing 60 nmol Tris-HCl, pH 6.8, 5% sodium dodecyl sulfate, and 10% glycerol as described in Marques et al.[56] All samples were sonicated (Bioruptor, Diagnode) for 10 minutes and prepared for Western blotting as previously described. For detection of C1INH protein, a polyclonal anti-C1INH antibody (CKBeR-2014) diluted 1:300 was used as primary antibody, and an HPR-conjugated anti-rabbit IgG (Agilent Technologies, P0448) diluted 1:10,000 was used as a secondary antibody. V5-tagged C1INH protein was detected using a monoclonal anti–V5-Tag antibody (Cell Signaling Technology, 13202) diluted 1:3,000 and an HPR-conjugated anti-rabbit IgG antibody (Agilent Technologies, P0448) diluted 1:10,000. β-Actin was detected using a monoclonal β-actin antibody (ab6276, Abcam) and an HPR-conjugated anti-mouse IgG antibody (Agilent Technologies, P0447).

Assays for C1INH–enzyme complexes

For ELISA measurements, C1INH samples were generated by transient transfection of HeLa cells. On day 1, the cells were seeded in 6-well plates at a density of 2×10^5 cells per well. At 24 hours after seeding, the cells were transfected with a total amount of up to 1350 ng plasmid DNA per well using Turbofect (Thermo Fisher Scientific). For separate measurements of C1INH proteins encoded by the *SERPING1* variants, HeLa cells were transfected with 900 ng pSERPING1[variant] per well. For measurements of coexpression of normal and mutated C1INH, HeLa cells were transfected with 450 ng pSERPING1[WT] and 450 ng pSERPING1[variant] per well. For dose–response assays, HeLa cells were cotransfected with 450 ng pSERPING1[WT], increasing amounts (50, 200, 450, 700, 900 ng) of pSERPING1 [variant], and pcDNA to a final amount of 1350 ng plasmid DNA per well. At 24 hours after transfection, the supernatant was removed, the cells were washed with PBS, and 1 mL Opti-MEM (Thermo Fisher Scientific) was added to the wells. At 48 hours after renewing the medium, the supernatant was collected for ELISA. The supernatant was spun down and transferred to a new tube to avoid the transfer of dead cells. To test the ability of the C1INH variants to form complexes with proteases, the supernatant samples were subsequently incubated with an excess of one of the target proteases pKa or mannan-binding lectin serine protease 1 (MASP-1). The pKa and MASP-1 concentrations required to create excess of target protease were initially established according to test measurements of supernatant samples from HeLa cells transfected with vectors encoding WT *SERPING1* (data not shown).

For C1INH-pKa complex formation in samples of separately expressed C1INH variants, C1INH samples were diluted 1.5 times (TBS, 0.1% Tween 20, 1% BSA) and incubated with an equal volume of 5 μg/mL pKa (Enzyme Research Laboratories, HPKa 1303) for 1 hour at 37°C. For complex formation between separately expressed C1INH variants and MASP-1, undiluted C1INH samples were incubated with an equal volume of 5 μg/mL MASP-1 (the activated MASP-1 used is described as "MASP1 EK" by Pihl et al[57]) for 2.5 hours at 37°C. For C1INH-pKa complex formation in samples with coexpression of *SERPING1* variants, C1INH samples were diluted 16 times (TBS, 0.1% Tween 20, 1% BSA) and incubated with an equal volume of 3 μg/mL pKa for 1 hour at 37°C to a final dilution of ×32.

We tested for the formation of C1INH-enzyme complexes, essentially following the recommendations in Kajdácsi et al.[58] Microtiter wells (96-well polystyrene flat-bottom MicroWell MaxiSorp plates, Thermo Fisher Scientific) were coated with capture C1INH reacting nanobody 1B12 (diluted in PBS) overnight at 4°C. The plates were coated with 5 μg/mL 1B12 for measurements on separately expressed *SERPING1* variants, and 2.5 μg/mL 1B12 for measurements of coexpressed *SERPING1* variants. The next day, the wells were blocked (TBS, 0.5% Tween 20, 3% BSA) for 2 hours at room temperature on a rocking table. Then 50 μL sample per well was loaded in the wells and incubated at room temperature for 1 hour on a rocking table. After incubation, the wells were rinsed (TBS, 0,05% Tween 20), and 50 μL per well detection antibody was added to the wells and incubated for 1 hour on a rocking table at room temperature. For the C1INH-pKa complex ELISA, a polyclonal anti-prekallikrein antibody (Cedarlane Laboratories) was used for detection (1:2000 in TBS + 0.1% Tween 20 + 1% BSA). For the C1INH–MASP-1 complex ELISA, a monoclonal anti–MASP-1 antibody (5A6B7, described in Troldborg et al[59]) was used for detection (1 μg/mL in TBS + 0.1% Tween 20 + 1% BSA). Next, the plates were rinsed (TBS, 0.005% Tween 20) and incubated with

peroxidase-conjugated polyclonal rabbit anti-goat immunoglobulins (Agilent Technologies Dako, 1:4000 in TBS + 0.1% Tween 20 + 1% BSA) for the C1INH-pKa complex ELISAs or peroxidase-conjugated polyclonal goat anti-mouse immunoglobulins (Agilent Technologies Dako, 1:4000 in TBS + 0.05% Tween 20 + 1% BSA) for the C1INH–MASP-1 complex ELISAs for 1 hour at room temperature on a rocking table. Finally, the wells were rinsed (TBS + 0.005% Tween 20) and developed by adding 50 μL per well of Ultra TMB-ELISA substrate solution (Thermo Fisher Scientific, 34028). Substrate conversion was stopped by adding 25 μL per well H_2SO_4 (0.2 mol). Absorbance was measured at 450 nm.

Confocal microscopy

For visualization of intracellular C1INH, confocal microscopy was carried out. On day 1, HeLa cells were seeded in 6-well plates at a density of 1×10^5 cells per well. At 24 hours after seeding, the cells were transfected using Turbofect (Thermo Fisher Scientific). For visualization of C1INH encoded by separately expressed *SERPING1* variants, HeLa cells were transfected with 900 ng pSERPING1[variant]. For visualization of normal C1INH when coexpressed with mutated C1INH, HeLa cells were transfected with 450 ng pSERPING1[WT]-V5 and 450 ng pSERPING1 [variant]. In both the separate and coexpressing studies, 200 ng of an expression plasmid encoding Tomato-Calreticulin was included in the transfection to visualize the ER. For the validation studies in Fig E6, HeLa cells were transfected with 450 ng pSERPING1[WT]-mCherry and 450 ng pSERPING1[variant]. On day 3, the transfected cells were moved to collagen-coated (Sigma-Aldrich) coverslips (VWR, 631-0125). On day 5, the cells were fixed for 10 minutes in 4% paraformaldehyde (Thermo Fisher Scientific) and washed 3 × 3 minutes with PBS.

For the separately expressed *SERPING1* variants, transfected HeLa cells were kept in ice-cold 70% ethanol in the freezer and washed 3 × 3 minutes (PBS). The presence of C1INH was visualized with an anti-C1INH polyclonal primary antibody (PA513627, Invitrogen) diluted 1:50 (PBS, 3% BSA). This was followed by 3 × 3 minute wash (PBS) before the primary C1INH antibody was labeled with Alexa Fluor 647–conjugated secondary antibody (Thermo Fisher Scientific) diluted 1:400 (PBS, 3% BSA). For staining of nucleic acids, 2 μg/mL Hoechst (Sigma-Aldrich, B2261) was added to the dilution of the secondary antibody. After staining, the coverslips were washed in PBS and mounted on microscope slides with Glycergel mounting medium (Agilent Technologies Dako). The cotransfected HeLa cells were, after fixation in 4% paraformaldehyde, permeabilized (PBS, 0.2% Triton X-100; Sigma-Aldrich) for 10 minutes and then blocked (PBS, 2% BSA) for 1 hour. Then the cells were washed 2 times (PBS, 0.05% Triton X-100) before the cells were stained with a monoclonal anti–V5-Tag primary antibody (Cell Signaling Technology, 13202) diluted 1:400 (PBS, 1% BSA, 0.05% Triton X-100). This was followed by 3 × 5 minute wash (PBS, 0.05% Triton X-100) before labeling of primary anti–V5-tag antibody with Alexa Fluor 647–conjugated secondary antibody (Thermo Fisher Scientific) diluted 1:400 (PBS, 1% BSA, 0.05% Triton X-100). After staining with the secondary antibody, the cells were washed 3 × 5 minutes (PBS, 0.05% Triton X-100) and 2 times with ddH_2O. For visualization of nucleic acids, the cells were stained with 0.5 μg/mL 4′,6-diamidino-2-phenylindole (aka DAPI; Thermo Fisher Scientific, D1306). After the nucleic acid staining, the coverslips were washed in ddH_2O and mounted on microscope slides with Glycergel mounting medium (Agilent Technologies Dako). The cells in the validation study cotransfected with pSERPING1 [WT]-mCherry and pSERPING1[variant] were, after fixation, directly mounted on microscope slides. No nucleic acid stain was included. The cells were imaged with a Zeiss LSM800 inverted confocal microscope equipped with a sensitive GaAsP detector, 3 detectors, 1 Zeiss Airyscan detector, 1 transmitted detector, and a Plan-Apochromat 63×/1.40 Oil DIC M27 objective. Airyscan image processing was performed by Zeiss's Zen Desk software.

Flow cytometry

To investigate cell viability after coexpression of normal C1INH and C1INH encoded by the studied *SERPING1* variants, flow cytometry was carried out. On day 1, HeLa cells were seeded in 6-well plates at a density of 2×10^5 cells per well. At 24 hours after seeding, the cells were cotransfected with 450 ng pSERPING1[WT] and 450 ng pSERPING1[variant] using Turbofect (Thermo Fisher Scientific), and 24 hours after transfection the growth medium was renewed. At 72 hours after transfection, the cells were collected and prepared for flow cytometry. Cell pellets were resuspended in fluorescence-activated cell sorting buffer ($PBS^{-\prime}-$, 2% fetal bovine serum, 2 mmol EDTA) and transferred to a 96-well plate containing propidium iodide to a final concentration of 1.25 μg/mL to identify dead cells. Fluorescence was quantified on a NovoCyte 2100 flow cytometer (Agilent).

Heat map

Numerical data from ELISA and Western blot quantified using ImageJ were used together with categorical data for whether foci were observed by microscopy of cotransfected samples. The Western blot data was $\log_2$ transformed. The data for all experiments were mean normalized by subtracting the mean and dividing by the standard deviation for each experiment. The heat map function in R v4.0.2 was used to create the heat map, with 'hclust' package used to perform hierarchical clustering.

RESULTS

Expression and secretion of C1INH proteins encoded by HAE-causing *SERPING1* gene variants

A panel of 28 different *SERPING1* variants reported to cause C1INH-HAE (Fig 1, *A*, Table I) were selected from the literature. Because we wanted to investigate gene variants encoding proteins with potential influence on normal C1INH protein produced from the WT allele, we deliberately biased our selection of gene variants by not including variants encoding severely truncated C1INH. We included published disease-causing alleles harboring missense variants, smaller in-frame deletions, or splice-site defects, which did not affect the reading frame. Many of the C1INH variants harbored amino acid substitutions that were found in positions scattered throughout the protein structure (Fig E1). However, common to the *SERPING1* variants included in the study was that they (1) encoded full-length or near full-length C1INH protein, (2) did not contain alterations in the region encoding the RCL, and (3) did not contain premature translation termination codons. Hence, these inclusion criteria excluded

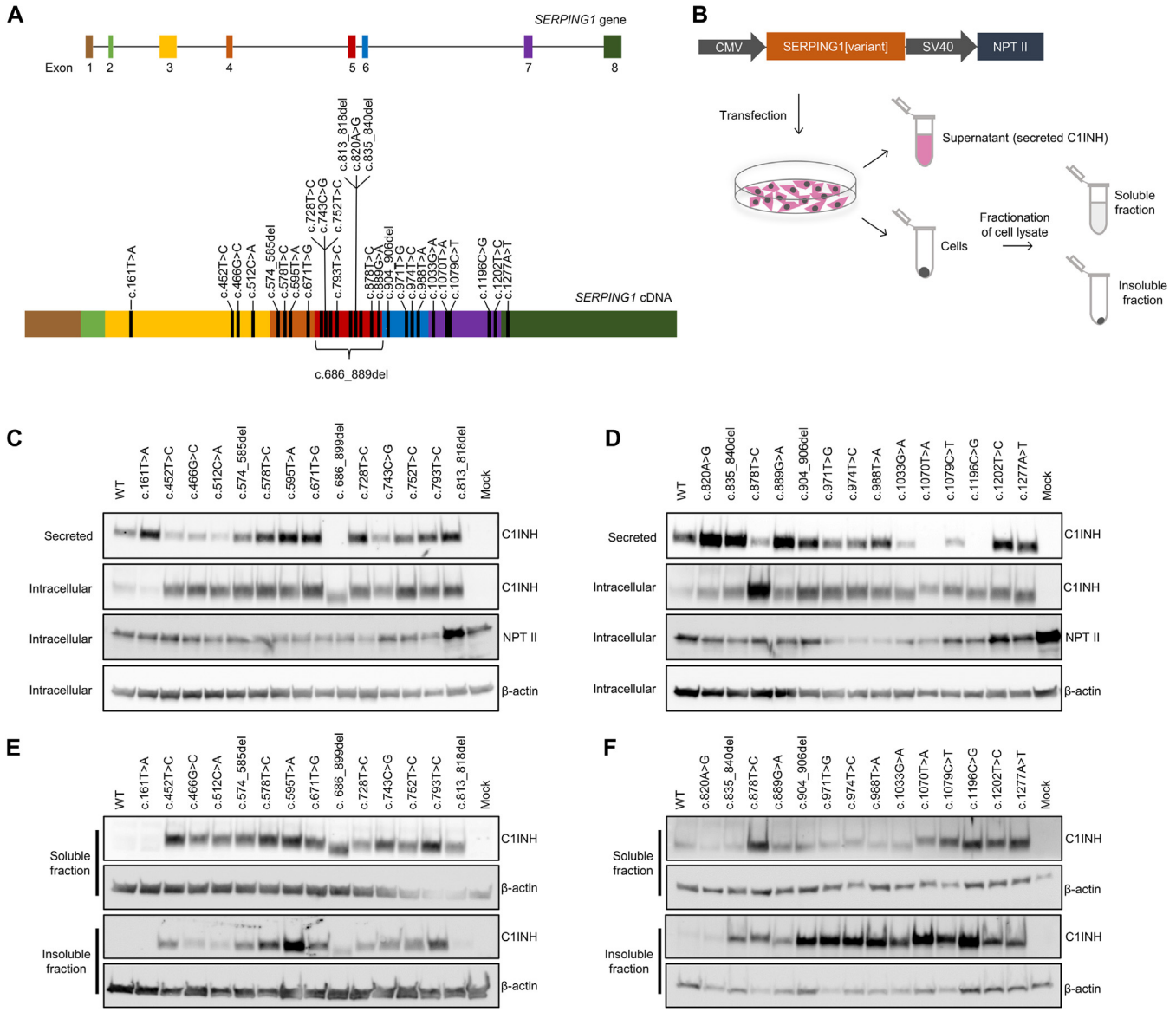

FIG 1. Intracellular and extracellular expression characteristics for studied *SERPING1* variants. **(A)** Schematic representation of *SERPING1* variants and their localization in *SERPING1* cDNA. **(B)** Schematic representation of experimental setup used in *(C-F)*. (**C** and **D**) Western blot analysis of C1INH secreted into supernatant and whole protein lysate. HeLa cells were transfected with 900 ng pSERPING1[variant], and protein was analyzed 72 hours after transfection. (**E** and **F**) Western blot analysis of soluble and insoluble protein fractions. After cell lysis, resulting protein was separated into soluble and insoluble fractions. β-Actin was used as loading control. Transfections in *(C-F)* were carried out in triplicate, and similar results were seen in at least 3 independent experiments.

variants carrying large deletions, variants located to the RCL, or variants with premature stop codons from our analysis. On the basis of the spectrum of *SERPING1* variants listed in ClinVar (www.ncbi.nlm.nih.gov/clinvar), counting more than 400 gene variants, it is estimated that more than 50% of the registered variants encode full-length or near full-length C1INH in which the reading frame is not affected. A set of expression constructs encoding the entire panel of selected *SERPING1* variants were then constructed. Expression of C1INH from these plasmids was driven by a cytomegalovirus promoter, whereas neomycin phosphotransferase was expressed from a flanking expression cassette containing the NPT II gene driven by a SV40 promoter (Fig 1, *B*).

First, we wanted to study the different C1INH proteins encoded by the *SERPING1* variants in a cellular context in the absence of normal C1INH protein. For this purpose, expression plasmid encoding each of the C1INH variants was transfected separately into HeLa cells, and amounts of secreted and intracellular C1INH protein were investigated by Western blot analysis (Fig 1, *C* and *D*). Cells transfected with plasmid that did not carry a *SERPING1* cDNA cassette were included as a negative control (mock). For all HAE-causing *SERPING1* variants, we found that C1INH protein was indeed produced after transfection of HeLa cells, and for all variants except for 3 (SERPING1[c.686_899del], SERPING1 [c.1070T>A] and SERPING1[c.1196C>G]), encoded C1INH was

TABLE I. Panel of 28 different *SERPING1* variants causing C1INH-HAE, selected from the literature

No.	*SERPING1* variant	Exon	Type of variant	Protein effect	Structural localization	Shown in Fig E1	C1INH protein length (residues)	Reference
—	WT	—	—	—	—	—	478	
1	c.161T>A	3	Missense	Leu32Gln	N-terminal domain	—	478	77
2	c.452T>C	3	Missense	Leu129Pro	hA	C	478	69
3	c.466G>C	3	Missense	Ala134Pro	hA	C	478	77
4	c.512C>A	3	Missense	Pro149Gln	hB	C	478	77
5	c.574_585del	4	Deletion	Asn170_173Serdel	hC	C	474	78
6	c.578T>C	4	Missense	Leu171Pro	hC	C	478	79
7	c.595T>A	4	Missense	Tyr177Asn	Between hC/hD	C	478	79
8	c.671T>G	4	Missense	Ile202Ser	S2A	B	478	79
9	c.686_899del	5	Splice	Asp207_274Serdel	hE/s1A/hF/s3A	D	410	79
10	c.728T>C	5	Missense	Leu221Pro	hE	B	478	77
11	c.743C>G	5	Missense	Pro226Arg	Between hE/hF	B	478	79
12	c.752T>C	5	Missense	Leu229Pro	Between hE/hF	B	478	80
13	c.793T>C	5	Missense	Trp243Arg	hF	B	478	81
14	c.813_818del	5	Deletion	Asn249_Asn250del	Between hF/s3A	B	476	82
15	c.820A>G	5	Missense	Ile252Val	Between hF/s3A	B	478	83
16	c.835_840del	5	Deletion	Asp257_Ser258del	Between hF/s3A	B	476	78
17	c.878T>C	5	Missense	Ile271Thr	sA3	B	478	84
18	c.889G>A	5	Missense	Ala275Thr	s3A	B	478	78
19	c.904_906del	6	Deletion	Thr280del	Between s3A/s4C	D	477	84
20	c.971T>G	6	Missense	Met302Arg	s3C	D	478	77
21	c.974T>C	6	Missense	Met303Thr	s3C	D	478	85
22	c.988T>A	6	Missense	Tyr308Asn	s3C	D	478	77
23	c.1033G>A	7	Missense	Gly323Arg	s2B	C	478	79
24	c.1070T>A	7	Missense	Ile335Asn	s3B	C	478	77
25	c.1079C>T	7	Missense	Pro338Leu	s3B	C	478	69
26	c.1196C>G	7	Missense	Pro377Arg	s2C	D	478	79
27	c.1202T>C	7	Missense	Ile379Thr	Between s2C/s6A	B	478	69
28	c.1277A>T	8	Missense	Asn404Ile	Between s5A/hI	C	478	69

to some extent secreted into the supernatant. Notably, relative to normal C1INH protein expressed from plasmid containing the unmodified *SERPING1* sequence, an increase of the intracellular level of C1INH protein was observed for all variants except for SERPING1[c.161T>A] (quantification in Fig E2, *A*). For 9 of the variants, the increase in intracellular C1INH protein was accompanied by a decrease in secreted C1INH (quantification in Fig E2, *B*). This supports our earlier observations that C1INH encoded by disease-causing *SERPING1* variants is less effectively processed and/or transported relative to normal C1INH.[48] To ensure that differences in total C1INH protein did not reflect differences in transfection efficiency between the different *SERPING1* variants, the level of neomycin phosphotransferase (NPT II) was determined. Although some variation of intracellular NPT II levels was observed for a few samples (Fig 1, *C* and *D,* and Fig E2, *C*), we conclude that differences observed in the levels of C1INH did not reflect transfection variation.

Differences in solubility between C1INH proteins encoded by HAE-causing *SERPING1* variants

Studies of the archetype serpin α_1 antitrypsin (A1AT, encoded by *SERPINA1*) have shown that normal A1AT and mutant pathogenic A1AT segregate differently during cell lysis for preparation of protein. Normal A1AT is primarily present in the soluble fraction, whereas mutated A1AT is present in higher amounts in the insoluble fraction.[60,61] The presence of the proteins in distinct fractions potentially reflect differences the intracellular processing. To examine and compare the solubility of plasmid-encoded C1INH variants, intracellular proteins in transfected cells were separated into a soluble and an insoluble fraction (Fig 1, *B*), and the level of C1INH protein was estimated in both fractions (Fig 1, *E* and *F*). Notably, for all selected *SERPING1* variants except SERPING1[c.161T>A], higher amounts of C1INH protein were detected in the insoluble fraction relative to cells transfected with plasmid encoding normal C1INH (Fig 1, *E* and *F,* and Fig E2, *D*). These data support the notion that full-length or near full-length C1INH encoded by the selected panel of disease-causing *SERPING1* variants is processed differently in cells than normal C1INH.

Colocalization of C1INH protein encoded by disease-causing *SERPING1* variants with ER in a pattern similar to normal C1INH protein

To further investigate potential differences in cellular localization and solubility, confocal microscopy was carried out on transfected HeLa cells using an anti-C1INH antibody to visualize C1INH protein (Fig 2). Cells were cotransfected with 900 ng pSERPING1[variant] and 200 ng of a plasmid encoding the Tomato fluorescence gene fused to a sequence encoding calreticulin (Tomato-Calreticulin) to visualize the ER. In cells transfected with pSERPING1[WT], the C1INH signal was evenly distributed in a pattern resembling the ER structure (Fig E3). No apparent differences in intracellular localization of C1INH or ER structure

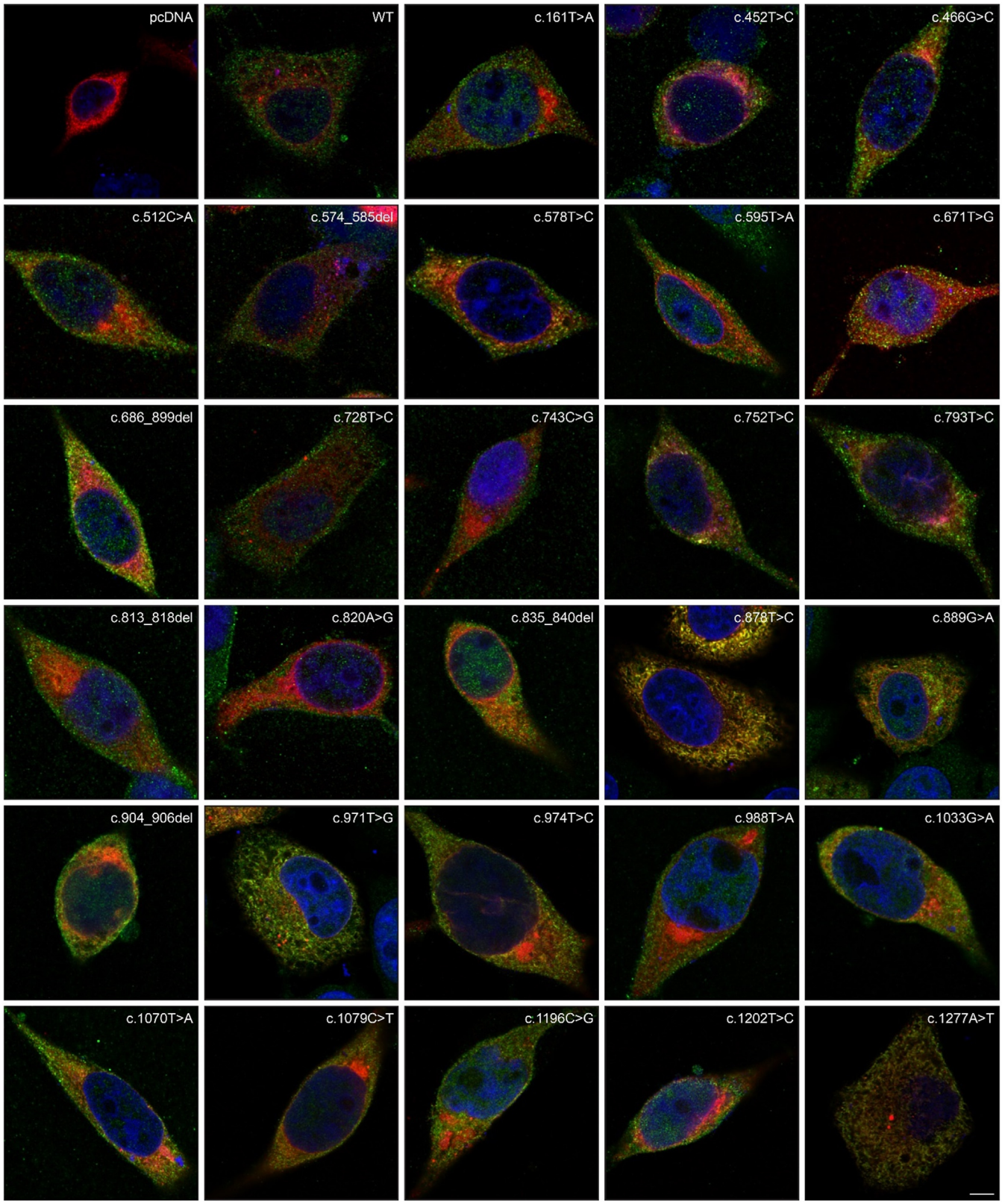

FIG 2. Intracellular localization of C1INH detected by confocal microscopy. HeLa cells were transfected with 900 ng pSERPING1[variant] and 200 ng of expression plasmid encoding Tomato-Calreticulin to visualize ER (Fig E3). At 72 hours after transfection, cells were fixed, and C1INH protein was visualized by anti-C1INH antibody *(green).* Scale bars: 5 μm. Representative images are shown.

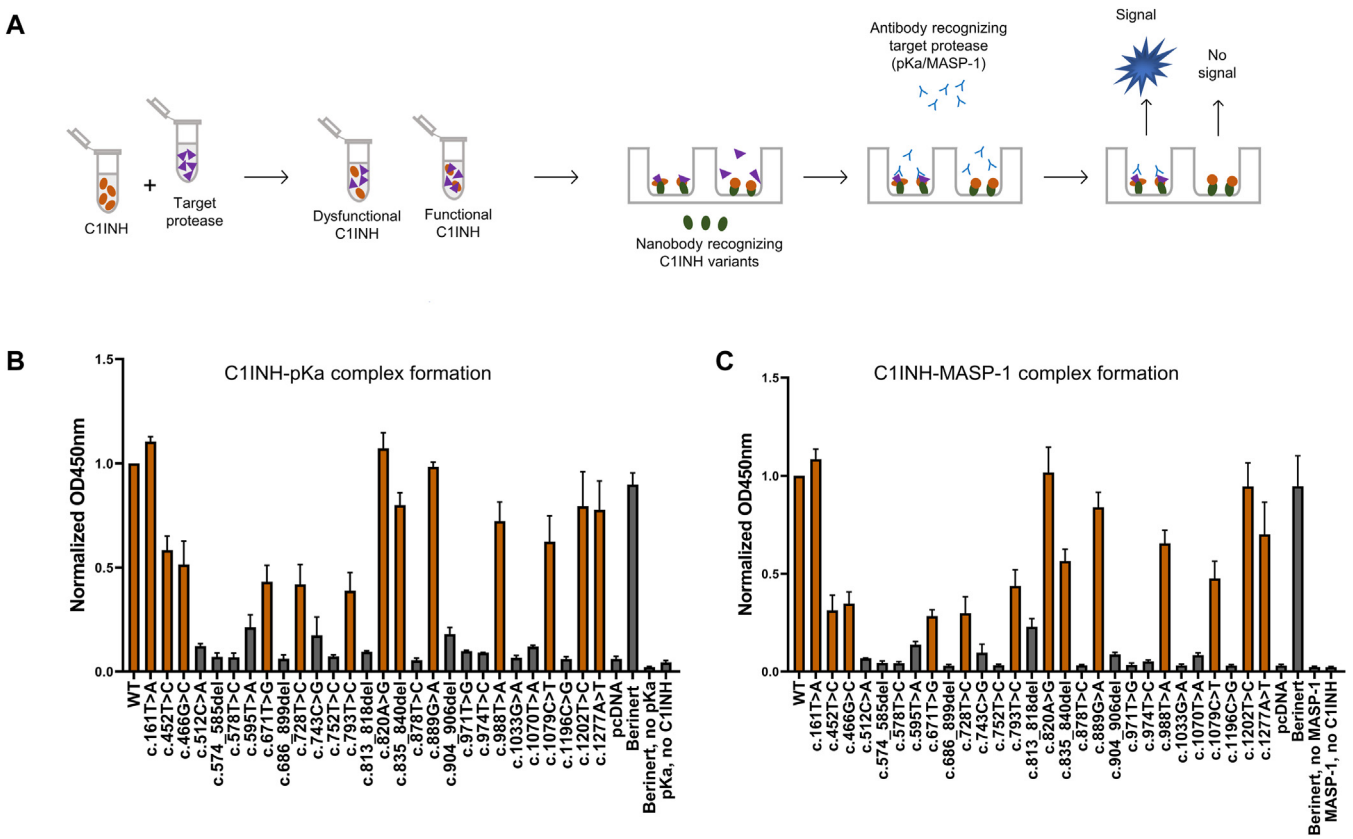

FIG 3. C1INH complex formation with target proteases pKa and MASP-1. **(A)** Schematic representation of experimental setup used in *(B)* and *(C)*. HeLa cells were transfected with 900 ng pSERPING1[variant]. At 72 hours after transfection, supernatant was collected. C1INH-containing supernatant was then incubated with excess of target protease for 1-2 hours at 37°C before being loaded onto ELISA plates. A nanobody recognizing C1INH variants was used for capture and either a pKa or MASP-1 antibody for detection. **(B)** C1INH-pKa complex ELISA. **(C)** C1INH–MASP-1 complex ELISA. Data in *(B)* and *(C)* represent means ± SDs of 3 independent experiments performed in technical duplicates.

were observed between cells transfected with pSERPING1[WT] and cells expressing the panel of disease-causing variants (Fig 2). On the basis of these findings, increased insolubility—and, for some variants, reduced levels of secretion—could not be linked directly to distinct intracellular localization profiles in cells expressing each variant alone.

Varying capacity of *SERPING1*-encoded C1INH protein to form complexes with plasma kallikrein and mannan-binding lectin serine protease 1

C1INH expressed from all but 3 of the studied *SERPING1* variants were secreted, resulting for several variants in higher levels of secreted C1INH relative to normal C1INH (Fig E2, *B*). To determine the functionality of secreted C1INH encoded by the complete set of *SERPING1* variants that were selected for this study, we utilized an immunoassay to test the ability of C1INH to form complexes with 2 C1INH serine protease targets: pKa and MASP-1. Supernatant from HeLa cells transfected with pSERPING1[variant] was collected after transfection and incubated with an excess of pKa or MASP-1 before quantification of complex formation. Plasma-derived C1INH concentrate (Berinert, CSL Behring) was included as a positive control. In the assay, C1INH is captured in microtiter wells by a C1INH-specific nanobody[62] and either a pKa or MASP-1 antibody used for detecting the presence of the 2 proteases, indicative of complex formation with C1INH (Fig 3, *A*).

Because the C1INH proteins encoded by the different *SERPING1* variants in the selected panel were secreted to a variable extent, it was not possible to utilize these assays to directly compare the activity of the different C1INH variants. Nonetheless, these experiments provided a key qualitative measure of the capability of secreted C1INH to form complexes with pKa and MASP-1. As shown in Fig 3, *B,* C1INH derived from almost half of the studied *SERPING1* variants was capable of forming complexes with pKa (Fig 3, *B, orange bars*). However, for the remaining 12 *SERPING1* variants, secreted C1INH was unable to form complexes with pKa, suggesting that C1INH produced by these variants was not functional. As expected, complexes with pKa were not formed for the 3 *SERPING1* variants encoding C1INH that were not secreted from the cells. To verify that samples reaching high optical density levels were not misinterpreted as a result of saturation of the assay, the samples were further diluted (Fig E4, *A*). Also, by performing the same analysis without adding pKa, it was verified that the pKa antibody did not recognize any of the C1INH variants directly (Fig E4, *B*).

To analyze for C1INH complex formation with MASP-1, we performed a similar set of analyses. Notably, detection of

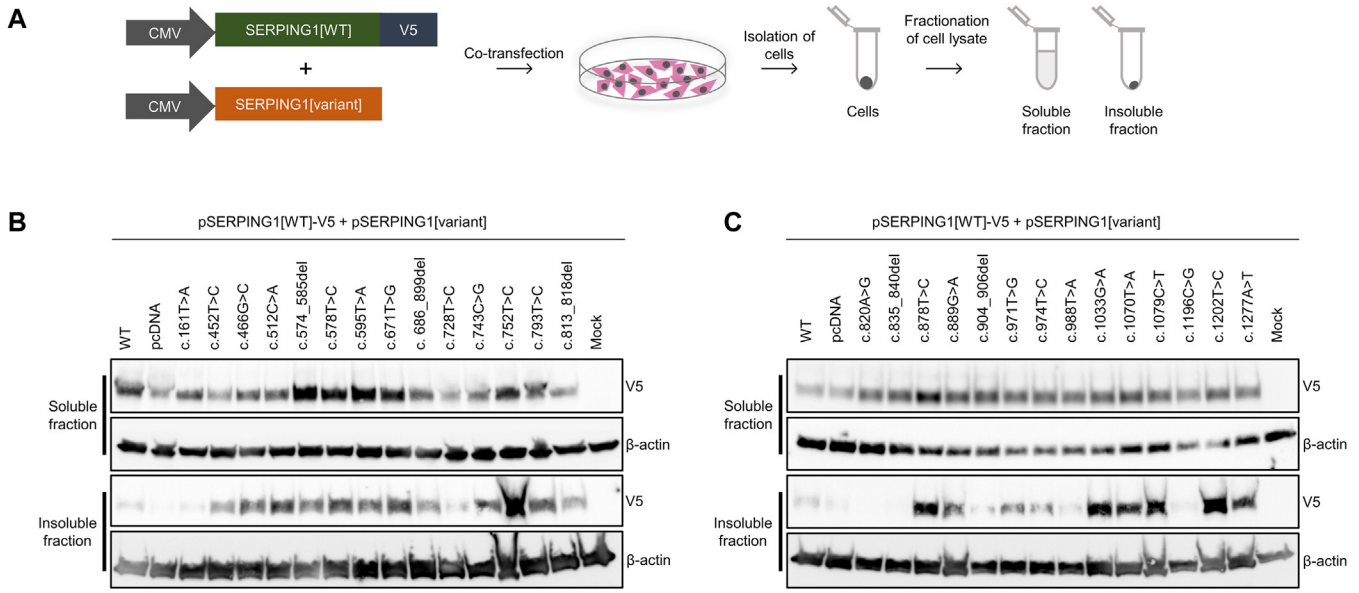

FIG 4. Coexpression of normal and mutated C1INH proteins change intracellular localization of normal C1INH protein. **(A)** Schematic representation of experimental setup used. HeLa cells were cotransfected with 450 ng pSERPING1[WT]-V5 and 450 ng pSERPING1[variant]. At 72 hours after transfection, supernatant and cells were collected for analysis. After cell lysis, resulting protein was separated into a soluble and insoluble fraction. **(B** and **C)** Western blot analysis of normal V5-tagged C1INH protein in soluble and insoluble proteins fractions. β-Actin was used as loading control. Transfections in *(B)* and *(C)* were carried out in triplicate, and similar results were seen in at least 2 independent experiments.

C1INH–MASP-1 complex formation unveiled a similar pattern (Fig 3, *C*), demonstrating that C1INH variants that were able to form complexes with pKa also formed complexes with MASP-1 (Fig 3, *C, orange bars*). Complex formation was not detected using an inactive MASP-1 variant (Fig E4, *C*) or in the absence of MASP-1 (Fig E4, *D*). Altogether, these data defined a group of 12 C1INH variants that were secreted but unable to bind target serine proteases.

Impact on subcellular localization of normal C1INH by C1INH expressed from disease-causing *SERPING1*

Our previous findings supported the notion that a subset of *SERPING1* variants causing HAE may have direct impact on the secretion and intracellular localization of C1INH produced from the WT *SERPING1* allele.[48] To mimic the situation in patient cells, we coexpressed each of the C1INH variants with normal C1INH and analyzed a possible effect on the solubility of the normal C1INH protein. HeLa cells were cotransfected with 2 plasmids, pSERPING1[WT]-V5 encoding V5-tagged normal C1INH and pSERPING1[variant] encoding an untagged C1INH variant. We then collected the cells and separated intracellular protein into a soluble and an insoluble fraction (Fig 4, *A*) and visualized normal C1INH protein by Western blot analysis using an anti-V5 antibody (Fig 4, *B* and *C*). Notably, transfection of HeLa cells with pSERPING1[WT]-V5 and either pSERPING1 [WT] or pcDNA resulted only in a faint band in the insoluble fraction. However, when pSERPING1[WT]-V5 was cotransfected with the selected disease-causing *SERPING1* variants, more than twice the amount of normal V5-tagged C1INH appeared in the insoluble fraction for 17 of the 28 variants (Fig E4, *E*), lending support to the notion that transport and secretion of normal C1INH were affected by coexpression of the majority of C1INH variants in the selected panel.

Induced formation of intracellular foci colocalizing with ER by C1INH encoded by a subset of *SERPING1* variants

To further investigate the changes in intracellular distribution of normal V5-tagged C1INH protein on coexpression with C1INH variants, we performed confocal microscopy on HeLa cells cotransfected with equal amounts of pSERPING1[WT]-V5 and pSERPING1[variant]. In HeLa cells coexpressing normal V5-tagged C1INH and untagged normal C1INH, normal V5-tagged C1INH was evenly distributed in the cells in a pattern resembling the ER structure. For a subset of the studied *SERPING1* variants (10 out of 28), we found that encoded C1INH changed the intracellular localization pattern of normal V5-tagged C1INH (Fig 5), resulting in formation of intracellular C1INH foci colocalizing with the ER (Fig E5). For further validation of this finding, the same experiment was carried out for focus-forming *SERPING1* variants using an mCherry tag instead of the V5 tag, again showing the formation of C1INH foci (Fig E6). These studies also validated the impact of SERPING1[c.551_686del], a variant that we have previously shown to trigger condensation of foci on cotransfection of normal and mutated C1INH.[48]

In summary, for a total of 10 variants, our data show formation of foci containing normal C1INH in the presence of mutated C1INH, indicating that normal V5-tagged C1INH protein is accumulating and held back within the ER as a direct consequence of the coexpression of C1INH variants. Notably, none of the variants induced focus formation when they were expressed alone (Fig 2), which aligns with the notion that C1INH encoded by a subset of *SERPING1* variants restricts the secretion

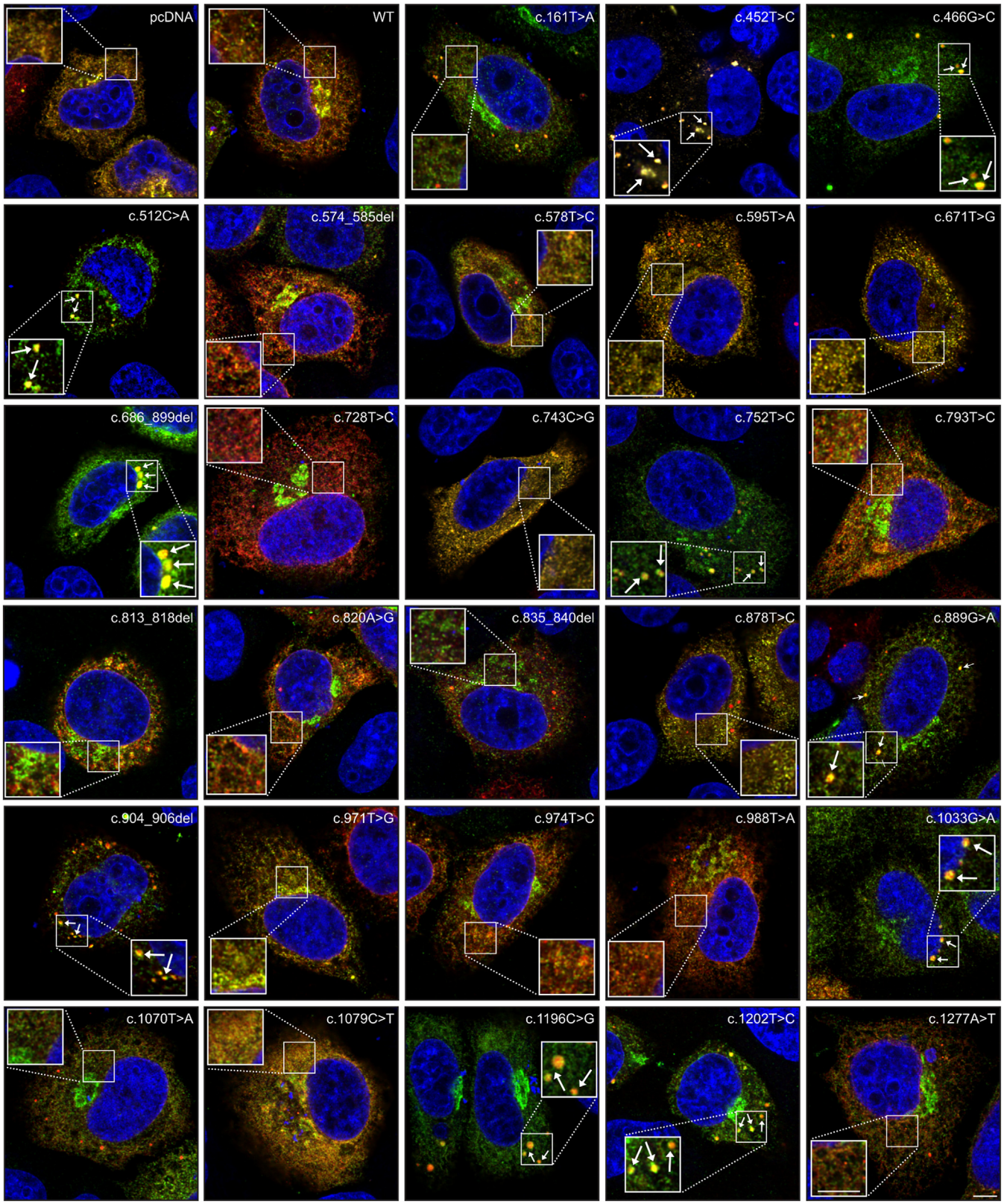

FIG 5. Formation of intracellular C1INH foci colocalizing with ER after coexpression of normal and mutated C1INH. HeLa cells were cotransfected with 450 ng pSERPING1[WT]-V5, 450 ng pSERPING1[variant], and 200 ng of expression plasmid encoding Tomato-Calreticulin to visualize ER (Fig E5). At 72 hours after transfection, cells were fixed, and normal V5-tagged C1INH was visualized using anti-V5 antibody *(green). Inset,* Formation of intracellular foci *(white arrows).* Scale bars: 5 μm. Representative images are shown.

of normal C1INH by the formation of intracellular aggregates colocalizing with the ER.[48]

Negative impact of coexpressed mutated C1INH on the functionality of normal C1INH

Next, we wanted to investigate if the impact of mutated C1INH on the intracellular localization and solubility of normal C1INH had a measurable impact on the overall activity of secreted C1INH. First, we investigated C1INH-pKa complex formation in the supernatant from cells coexpressing normal and mutated C1INH (Fig 6, *A*). Notably, the formation of C1INH-pKa complexes doubled on transfection of the cells with twice the amount of pSERPING1[WT] plasmid (relative to cells transfected with pSERPING1[WT] and pcDNA control plasmid), suggesting that complex formation was not saturated under the experimental conditions. For cells cotransfected with pSERPING1[WT] and either pSERPING1[c.161T>A] or pSERPING1[c.820A>G], complex formation increased 2-fold as well, whereas C1INH-pKa complex formation was most severely affected in the supernatant from cells cotransfected with pSERPING1[WT] and pSERPING1[c.1196C>G], reaching only ~40% of the complex formation observed with the pcDNA control. For cells coexpressing normal C1INH and C1INH encoded by pSERPING1 [c.835_840del], pSERPING1[c.889G>A], and pSERPING1 [c.1202T>C], the level of complex formation was slightly higher than for the control. C1INH encoded by the remaining *SERPING1* variants led to comparable or decreased C1INH-pKa complex formation in the supernatant compared to cells coexpressing normal C1INH or cells cotransfected with pcDNA. On the basis of the capacity of 13 of the 28 variants to form complexes with pKa and MASP-1 (Fig 3, *B* and *C*), one would expect that expression of all these 13 variants (and not just 3 of them: c.835_840del, c.889G>A, and c.1202T>C) would contribute to overall complex formation in the supernatant. To rule out that a potentially negative effect on cell viability caused by the coexpression of normal and mutated C1INH could explain this discrepancy, we analyzed the viability of transfected cells by flow cytometry, but we did not detect any differences in cell survival (Fig E7).

To study this phenomenon further, we performed a series of dose–response experiments in which HeLa cells were cotransfected with 450 ng pSERPING1[WT] and increasing amounts of pSERPING1[variant] (Fig 6). First, we tested the effect of 7 C1INH variants characterized by low secretion and lack of ability to form complexes with the 2 target proteases. For all these variants, we observed a gradual decrease in C1INH-pKa complex formation in supernatants from HeLa cells transfected with increasing amounts of plasmid DNA encoding *SERPING1* variants (Fig 6, *B*). This demonstrated that the C1INH protein encoded by these gene variants had a negative impact on normal C1INH protein. For the secreted but nonfunctional C1INH variants, C1INH-pKa complex formation stayed relatively stable, with increasing amounts of variant C1INH at a level that was only slightly decreased relative to the pcDNA control (Fig 6, *C*), indicating that C1INH protein encoded by these variants had minor or no impact on the activity of normal C1INH protein. One variant (c.574_585del), however, did seem to have an additive effect on overall complex formation (Fig 6, *C*).

For *SERPING1* variants encoding functional C1INH proteins, we first tested the impact of variants with low complex formation. For all 5 variants in this category, complex formation remained stable at a level comparable to the pcDNA control, suggesting that the expected additive effect on complex formation for these variants was not evident (Fig 6, *D*). This indicated that coexpression of these C1INH variants and normal C1INH had an overall negative impact leading to a lower-than-expected activity level. For functional C1INH variants characterized by medium complex formation (total of 6 variants), we found that C1INH-pKa complex formation increased to varying degrees with increasing amounts of plasmid DNA encoding the C1INH variants (Fig 6, *E*). For the remaining 2 variants, c.161T>A and c.820A>G, which in general performed like WT *SERPING1,* we confirmed an additive effect of coproducing normal and mutant C1INH (Fig 6, *F*). Together, these data demonstrate for most of the tested variants a level of combined activity, which is indicative of a negative impact of mutated C1INH on normal C1INH.

Negative effect of mutated C1INH on overall C1INH activity showing a prevalence of dominant-negative disease mechanisms

For each individual *SERPING1* variant, we measured the capacity to form complexes with pKa (Fig 3, *B*), allowing us to determine the relative complex-forming activity of each variant. On the basis of this analysis, we could estimate predicted complex formation under the assumption that the normal and mutated C1INH proteins had no effect on each other and apply such predictions for scenarios where C1INH variants were coexpressed from *SERPING1* WT and disease variants (cotransfections using equal amounts of plasmid DNA). Hence, complex formation was predicted for each sample by adding the predicted contribution from the normal C1INH protein (WT sample normalized to 1) to the expected contribution from the disease variant and compared to the measured complex formation, as determined in Fig 6, *A*. For easier interpretation of the data, the measured complex formation for each cotransfection was normalized to the corresponding predicted complex formation. On the basis of this analysis, it became evident that the actual C1INH-pKa complex formation capacity for 25 of 28 selected variants was reduced to 38-75% of the level that could be predicted for expressing WT and disease-causing *SERPING1* variants together (Fig 6, *G*). This demonstrates that a large fraction of the selected *SERPING1* disease variants encoding full-length or near full-length C1INH has a negative, rather than an additive or supportive, role on the overall C1INH activity, lending support to the conclusion that dominant-negative mechanisms are prevalent in C1INH-HAE.

Subdivision of *SERPING1* variants into 5 clusters, each sharing distinctive molecular characteristics

Despite the high frequency of *SERPING1* alleles acting negatively on the WT allele, our series of cellular assays unveiled a heterogenous set of *SERPING1* alleles encoding C1INH proteins with distinct secretion profiles, intracellular localization patterns, and capacities to form complexes with target proteases. To group the 28 alleles that were initially selected for this study, we created a heat map and phylogeny based on the 6 experimental parameters listed in Fig 7. This allowed us to divide the *SERPING1* variants into 5 different clusters, each consisting of variants sharing molecular characteristics.

Two disease variants exhibited WT-like behavior in the cellular assays (except for showing higher levels of secreted C1INH) and

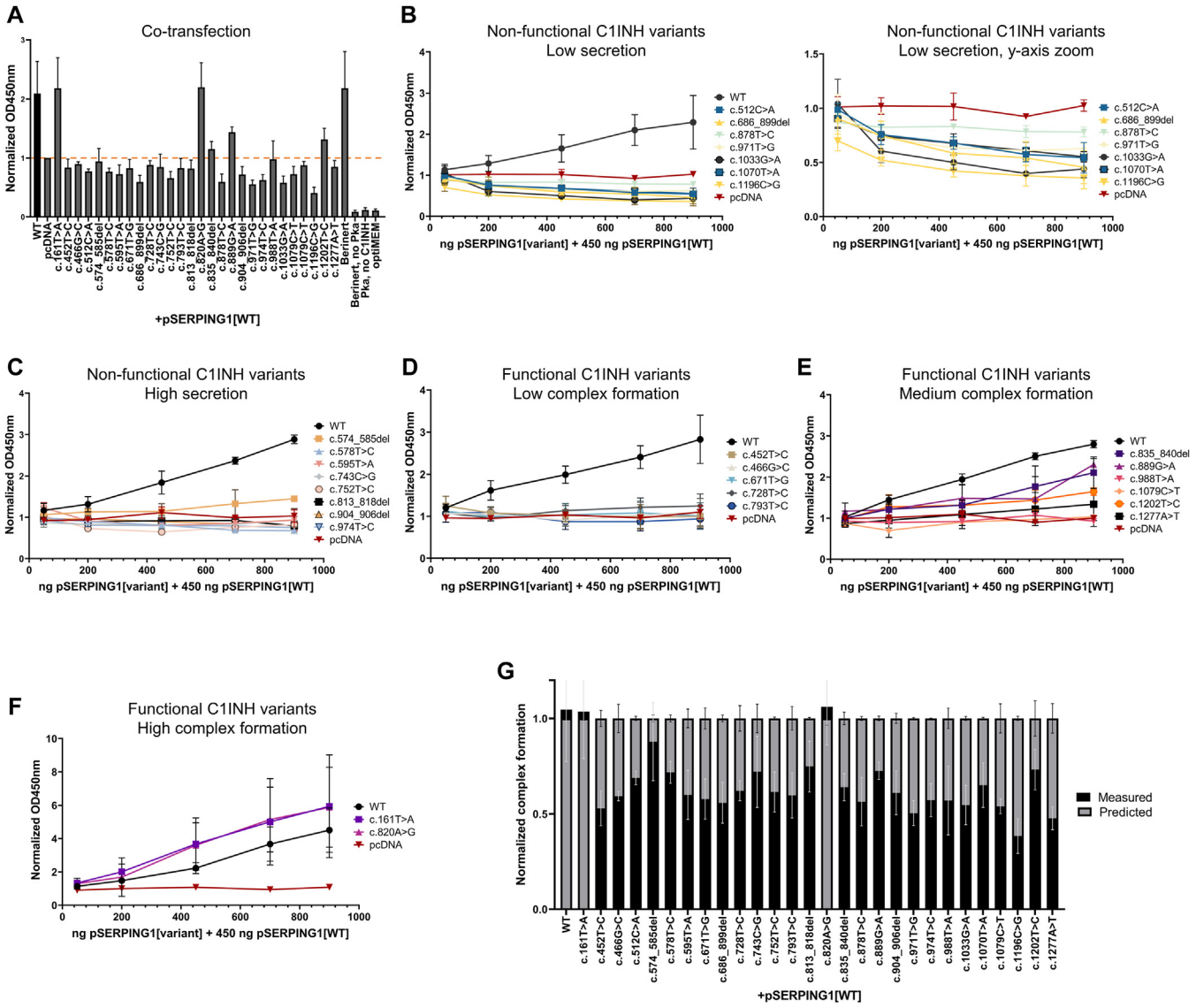

FIG 6. Negative impact on overall complex formation by coexpression of normal and mutated C1INH. **(A)** C1INH-pKa complex formation after coexpression of equal amounts of normal and mutated C1INH. HeLa cells were transfected with 450 ng pSERPING1[WT] and 450 ng pSERPING1[variant] or a pcDNA control plasmid. At 72 hours after transfection, supernatant was collected and incubated with target protease pKa at 37°C for 1 hour before being loaded onto ELISA plates. A nanobody recognizing C1INH variants was used for capture and anti-pKa antibody for detection. OD values were normalized to pSERPING1 [WT]/pcDNA sample. Data represent means ± SDs of 3 independent experiments performed in technical duplicates. **(B-F)** C1INH-pKa complex formation after coexpression of normal C1INH and increasing amounts of mutated C1INH. HeLa cells were cotransfected with 450 ng pSERPING1[WT] and increasing amounts of pSERPING1[variant] (50, 200, 450, 700, or 900 ng) and pcDNA to a final 1350 ng plasmid DNA per transfection. OD values were normalized to pSERPING1[WT]/pcDNA samples. Data represent means ± SDs of 3 independent experiments performed in technical duplicates. **(G)** Coexpression of normal and mutated C1INH has a negative impact on overall C1INH-pKa complex formation. Under the assumption that coexpression of normal C1INH and C1INH encoded by studied *SERPING1* variants had no impact on one another, predicted complex formation activity was estimated for each of cotransfections. Normalized OD values from Fig 3, *B,* were used. Expected complex formation for each cotransfection was estimated by adding expected contribution from C1INH variant (normalized OD values from Fig 3, *B*) to expected contribution from normal C1INH protein (WT samples normalized to 1). Measured C1INH-pKa complex formation was normalized OD values from Fig 6, *A*. Measured complex formation for each cotransfection was then normalized to corresponding predicted complex formation. *OD,* Optical density.

therefore clustered with WT *SERPING1* in cluster 1, separate from the remaining 26 *SERPING1* variants. Cluster 2 consists of 2 variants encoding C1INH that was secreted and capable of forming complexes with target proteases, but induced insolubility of normal C1INH and formation of intracellular C1INH foci. Common for the 8 *SERPING1* variants in cluster 3 was a reduced

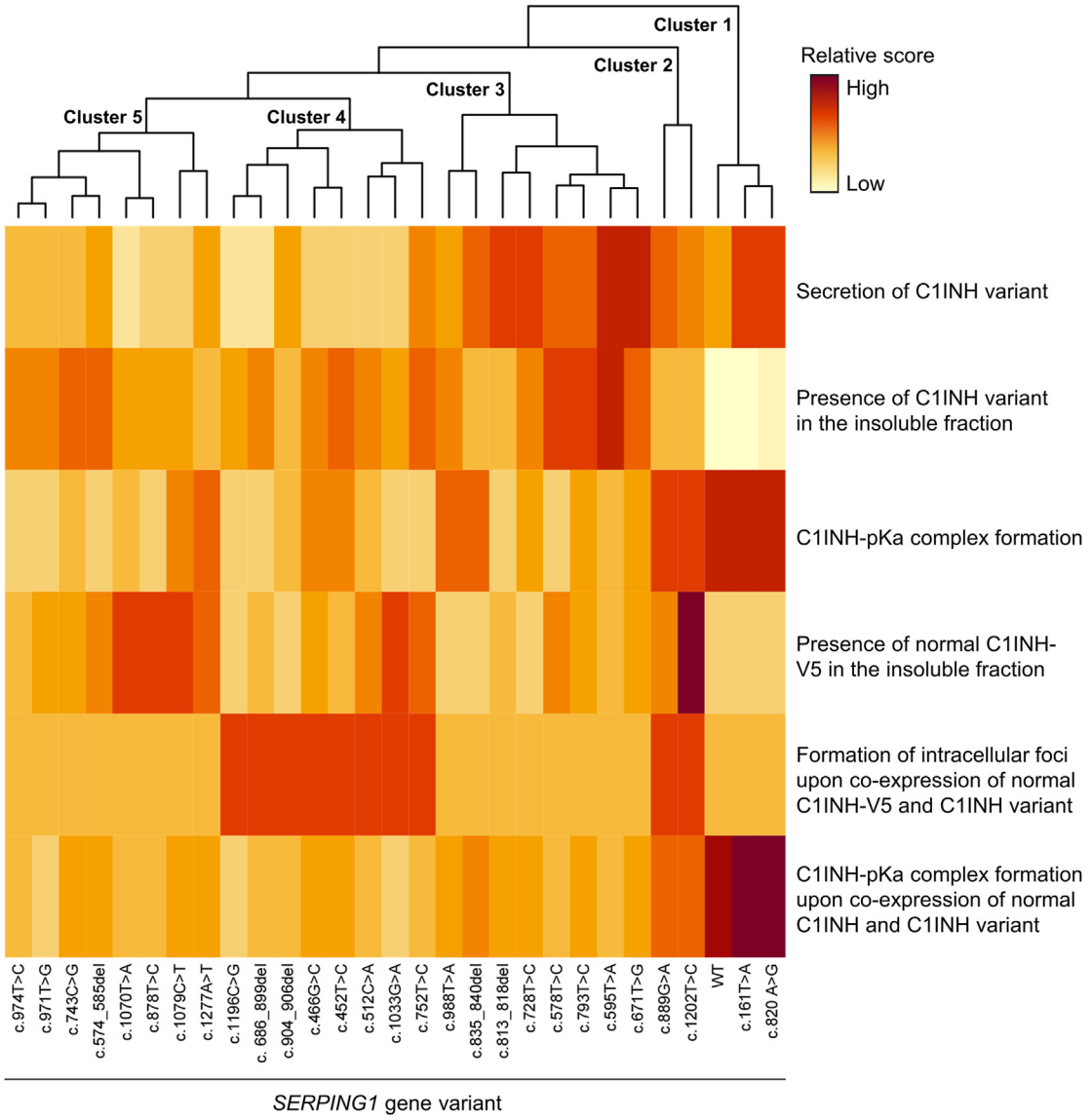

FIG 7. Classification of *SERPING1* variants based on subdivision into 5 clusters sharing distinct molecular characteristics. Heat map separating studied *SERPING1* variants into 5 clusters based on 6 parameters: *(i)* relative amount of secreted C1INH (Fig 1, *C* and *D,* Fig E2, *B*), *(ii)* relative amount of C1INH protein localized in insoluble fraction after cell lysis (Fig 1, *E* and *F,* and Fig E2, *D*), *(iii)* relative complex formation between C1INH variants and target protease pKa (Fig 3, *B*), *(iv)* relative level of normal C1INH-V5 protein localized in insoluble fraction after cotransfection of pSERPING1[WT] and pSERPING1[variant] (Fig 4, *B* and *C,* and Fig E4, *E*), *(v)* presence of intracellular C1INH foci after coexpression of pSERPING1[WT] and pSERPING1[variant] (Fig 5), and *(vi)* relative level of C1INH-pKa complex formation after cotransfection of pSERPING1[WT] and pSERPING1[variant] (Fig 6, *A*).

capacity of the encoded C1INH to form complexes with target proteases despite high expression and secretion. C1INH encoded by the variants was present in the insoluble protein fraction, and formation of foci was not evident by confocal microscopy. Common for all variants in cluster 4 was that they induced the formation of intracellular foci containing normal C1INH and had a negative impact on the overall complex formation with target protease pKa—both characteristics compatible with dominant-negative cellular disease mechanisms. The remaining 8 *SERPING1* variants grouped together in cluster 5, consisting of variants characterized by no or low secretion, but with the capacity to change the intracellular distribution of normal C1INH protein (increasing its presence in the insoluble fraction) without inducing detectable formation of C1INH foci as seen for the cluster 4 variants.

DISCUSSION

In the present study, we provide further insight into the complexity of the underlying molecular disease mechanisms in C1INH-HAE. We provide a new functional classification of *SERPING1* variants causing C1INH-HAE that is based on

molecular characterization of disease alleles, providing readouts on 6 functional parameters, including secretion potential, intracellular solubility, protease complex formation, and *trans*-acting impact on normal C1INH. Among a more or less randomly selected panel of 28 *SERPING1* variants encoding full-length or near full-length C1INH causing C1INH-HAE in heterozygous patients, we showed robust C1INH expression from all *SERPING1* variants. We found, however, that the intracellular solubility of disease-causing variants varied from that of normal C1INH, indicating that the cellular processing of mutant C1INH differed from that of normal C1INH. Still, C1INH encoded from nearly all *SERPING1* variants that were selected for this study was secreted into the supernatant, although to a varying extent. About half of the C1INH variants that were secreted to the supernatant were capable of forming complexes with target proteases, whereas the remaining secreted C1INH variants were dysfunctional. Notably, for the majority of the *SERPING1* variants, expression of mutant C1INH had an effect on the intracellular solubility of the normal C1INH protein, increasing its appearance in the insoluble fraction. Moreover, for 10 variants, coexpression of normal and mutant C1INH induced the formation of C1INH foci colocalizing with the ER. Our data also suggest that formation of protein foci that are detectable by microscopy does not necessarily correlate with the increased presence of protein in the insoluble protein fraction. Strikingly, for all examined variants but 2, the measured combined activity of mutant and normal C1INH was markedly lower than expected based on each individual variant's capacity to form complexes with target proteases (when expressed alone), suggesting a *trans*-acting negative effect of mutant C1INH. Together, our findings indicate that dominant-negative disease mechanisms are evident in C1INH-HAE. On the basis of the classification of *SERPING1* variants, such dominant-negative mechanisms are associated with at least 4 distinct C1INH protein profiles. It is important to note, however, that our selection of disease-causing *SERPING1* variants was biased toward variants more prone to having a dominant-negative effect. On the basis of the criteria that were initially used to select variants for this study, we excluded variants with altered reading frames and variants encoding severely truncated versions of C1INH, which would be less likely to interfere with normal C1INH protein.

Two of the studied *SERPING1* variants (SERPING1 [c.161T>A] and SERPING1[c.820A>G]) exhibited WT-like behavior and thus clustered with WT *SERPING1* in the phylogeny. Although we cannot exclude the notion that these variants possess alternative functional defects that could not be identified by our experimental design, we speculate that these variants are not singly responsible for the C1INH-HAE phenotype in patients carrying these variants. For the SERPING1[c.161T>A] variant encoding C1INH with a single amino acid change located in the N-terminal nonserpin domain, our data are consistent with previous studies showing that truncation of this section of the *SERPING1* gene does not affect secretion and functionality of the resulting C1INH protein.[63] For patients carrying these *SERPING1* variants, a specific combination of the *SERPING1* variant and unknown confounding factors may potentially support development of C1INH deficiency.

The remaining 26 *SERPING1* variants segregated from the WT into 4 separate clusters. Common for C1INH encoded by *SERPING1* variants in 2 of these clusters (clusters 2 and 4) was their ability to induce abnormal intracellular retention of C1INH in the ER, and these variants thus share a molecular hallmark of serpinopathies. The formation of protein polymers consisting of mutated serpins accumulating in the ER is well established for the serpinopathies A1AT deficiency (A1ATD) and familial encephalopathy with neuroserpin inclusion bodies (FENIB).[64-68] In regard to polymer formation, one notable characteristic of HAE is the composition of serpin polymers. In A1ATD and FENIB, the polymers have been found to consist of mutated proteins, whereas our observation is that C1INH polymer formation primarily occurs in cells coexpressing both normal and mutated C1INH protein.[48] This is also the case for the dominant-negative *SERPING1* variant reported by Yasuno and colleagues.[49] We have previously proposed that *SERPING1* variants with alterations possibly opening the protein structure at the shutter domain could allow the RCL of other C1INH proteins to insert here, thereby forming stable C1INH polymers.[48] Yet the underlying mechanism for C1INH polymer formation might be different depending on how the domain affected by the variant influences the structure of the C1INH protein. However, the molecular characteristics of the C1INH proteins triggering formation of C1INH foci differed between the 2 clusters. Hence, the 2 variants in cluster 2 encoded C1INH proteins that were efficiently secreted, capable of forming complexes with target proteases, and had an additive effect on the overall complex formation when coexpressed with WT *SERPING1*. For the two cluster 2 variants, formation of foci seemed to have less severe impact on the overall activity when coexpressed with normal C1INH, although our study design did not allow us to explain the mechanism behind this. C1INH encoded by the variants in cluster 4 was, in general, secreted to a lower extent. Most of these C1INH variants were incapable of forming complexes with target proteases and had either a negative or no impact on the overall complex formation with target proteases when coexpressed with normal C1INH. On the basis of the ability to induce formation of C1INH foci, it is tempting to draw the conclusion that C1INH encoded by these *SERPING1* variants results in pathogenic low C1INH plasma levels through intracellular retention of normal C1INH. However, our data indicate that the situation is potentially even more complex. Hence, coexpression of C1INH encoded by the variants in cluster 2 together with normal C1INH had an additive effect on the overall activity measured by complex formation with target proteases. Interestingly, the SERPING1[c.1202T>C] variant located in cluster 2 has been identified as disease causing both in a heterozygous and homozygous state in HAE patients.[69,70] However, we only observed foci in the mimicked heterozygous state. At this point, we cannot exclude the idea that our experimental setup did not allow sufficient time for larger foci to form, with a possible impact on the additive effect in the mimicked heterozygous state or in the mimicked homozygous state.

Six of the *SERPING1* variants in cluster 4 encode C1INH proteins that were either not secreted or were secreted as nonfunctional protease inhibitors. Coexpression of normal C1INH and C1INH encoded by these 6 *SERPING1* variants reduced the overall complex formation in the supernatant to 41-77% compared to cells expressing normal C1INH and a control vector. Thus, intracellular retention of normal C1INH through the formation of foci provided a possible explanation for low functional C1INH plasma levels in patients carrying these 6 *SERPING1* variants. C1INH encoded by the remaining 2 variants in cluster 4 was secreted, was capable of forming complexes with target proteases, and did not

reduce the overall complex formation compared to control when coexpressed with normal C1INH. As noted, we cannot exclude the idea that the timing in the experimental setup did not allow foci to be detected. Nevertheless, our data suggest that formation of C1INH foci for a subset of *SERPING1* variants is a key molecular disease mechanism contributing to and potentially even driving C1INH-HAE.

For the *SERPING1* variants in clusters 3 and 5, we did not detect the formation of C1INH foci, and aggregation of C1INH protein did not appear to drive disease development. However, we cannot exclude the possibility that these variants induced the formation of C1INH multimers that were not detectable by confocal microscopy. C1INH encoded by the variants in cluster 3 had a high expression profile and was present in the supernatant of transfected cells at comparable or increased levels compared to normal C1INH. Notably, despite the increased presence in the supernatant, complex formation was decreased relative to normal C1INH. For the secreted but dysfunctional C1INH proteins in cluster 3, this was expected. However, for the *SERPING1* variants for which complex formation with target proteases was observed, it can be speculated that these proteins are secreted in 2 conformations, functional and dysfunctional. The increased presence in the supernatant could also be explained by the encoded C1INH proteins adapting to a more stable but dysfunctional conformation. Although we observed that 5 of the *SERPING1* variants in cluster 3 produced C1INH protein that was secreted and to some extent capable of forming complexes with target proteases, only C1INH encoded by SERPING1[c.835_840del] had an additive effect on the overall complex formation when coexpressed with normal C1INH. This indicates that expression of C1INH from the disease allele has a negative impact on normal C1INH through mechanisms that are not yet known.

The *SERPING1* variants in cluster 5 encode C1INH proteins that were present at lower levels in the supernatant of transfected cells, and most of them were present in a conformation incapable of forming complexes with target proteases. Coexpression of normal C1INH and C1INH encoded by the *SERPING1* variants in cluster 5 changed the intracellular solubility of the normal C1INH protein, indicating that intracellular processing of the normal C1INH protein was affected by the presence of these C1INH variants. Interestingly, C1INH polymers have been found in the plasma of patients carrying the SERPING1[c.878T>C] variant[51] mapped to cluster 5. The significance of such polymers in relation to disease mechanisms remains unclear. However, the presence of extracellular C1INH polymers capable of activating the contact pathway could increase C1INH consumption in the plasma and thereby further reduce the C1INH plasma level. Extracellular polymers have also been found in both cell models and plasma samples from patients with A1ATD and FENIB.[71-73] The presence of extracellular C1INH polymers is a possible aspect in relation to C1INH-HAE molecular disease mechanisms that our study does not take into account.

Our study leads to the striking finding that a subset of HAE-causing *SERPING1* alleles encoding full-length or near full-length C1INH, including *SERPING1* variants encoding efficiently secreted C1INH, restricts the action of C1INH coexpressed from WT allele. Importantly, our findings were based on transfection experiments in HeLa cells, and we cannot exclude the notion that our data were influenced by the cell model. Hence, C1INH is primarily produced by hepatocytes in the liver and intracellular processing, including folding and secretion of the extensive range of altered C1INH proteins, could differ between HeLa cells and hepatocytes. However, we previously validated the *trans*-acting negative effect of a small subset of *SERPING1* variants in the human hepatocarcinoma cell line HepG2 using the same cellular assays and confirmed such findings in patient-derived fibroblasts.[48]

When we consider the tertiary structure of the C1INH protein (Fig E1), we find no apparent overlap between the localization of the C1INH alterations and the defined clusters. To identify a possible link between different molecular disease mechanisms and the structural localization of the *SERPING1* variants, an even more comprehensive study, including numerous HAE-causing *SERPING1* variants, would have to be carried out.

Different studies have sought to establish a correlation between the specific HAE phenotype and the *SERPING1* genotype, but without reaching obvious conclusions. The understanding of the disease mechanisms in C1INH-HAE is challenged by the phenotypic variability and incomplete penetrance, and the search for disease modulators has therefore now expanded into genes related to bradykinin metabolism. The F12-46C/T polymorphism has been associated with a less severe disease course in patients with C1INH-HAE.[74] Through next-generation sequencing of C1INH-HAE patients and healthy relatives from 31 families, Veronez et al[75] identified 211 genetic variants in 15 different genes related to the kallikrein-kinin system. However, a genotype-phenotype association could not be identified, and the authors alluded to the sample size and lack of functional studies as limiting factors. Increased C1INH metabolism has also been suggested to further lower the C1INH plasma levels in C1INH-HAE patients. Studies in plasma samples from C1INH-HAE patients and healthy controls have reached conflicting results, either measuring an increased C1INH catabolism[55] or finding the half-life of C1INH to be unaltered in C1INH-HAE patients compared to healthy individuals.[76] Our experimental setup does not account for the possible influence of such modifier genes, which might affect C1INH plasma levels through different mechanisms, including increased C1INH catabolism. Epigenetic and environmental factors could also be factors contributing to the molecular disease mechanisms in C1INH-HAE.

Our data, taken together, suggest that low C1INH plasma levels observed in C1INH-HAE patients reflect a number of molecular disease mechanisms. Most importantly, we find that coexpression of mutated C1INH and normal C1INH may have a restrictive impact on overall C1INH activity, even for variants that are actively forming complexes with proteases. It is obvious that reduced levels of C1INH leading to HAE may occasionally reflect haploinsufficiency, but our findings suggest that the lack of C1INH may in other cases reflect the negative impact of mutated C1INH on secretion of normal C1INH. Supported by previous findings demonstrating direct interactions between mutated and normal C1INH,[48] our data support the notion that interactions between coexpressed C1INH variants, even variants that are separately active and secreted, may in some cases restrict overall secretion. On the basis of the set of phenotypic readouts that was included in the study design, the data unveil molecular disease mechanisms that are not similar for all the studied *SERPING1* variants and thus provide, to our knowledge for the first time, a classification of C1INH-HAE–causing *SERPING1* variants based on specific functional readouts, allowing several clustering subgroups to be defined. Despite different functional properties of the studied C1INH variants, we demonstrate for

all but 2 variants a *trans*-acting negative impact of mutant C1INH on overall C1INH activity in cells coexpressing normal and mutant C1INH. These findings suggest that a large proportion of *SERPING1* alleles encoding full-length C1INH cause disease through dominant-negative mechanisms. Unraveling the molecular mechanisms underlying HAE is an important step in developing new treatments for C1INH-HAE, including potential new gene therapies. Hence, an important next step toward implementing gene therapies for treatment of C1INH-HAE will be to investigate the potential impact of dominant-negative *SERPING1* alleles in patients on the activity of C1INH effectively produced from gene therapy vehicles like recombinant adeno-associated virus-based vectors.

DISCLOSURE STATEMENT

Supported by CSL Behring, the Lundbeck Foundation, Fonden af 1870, Robert Wehnerts og Kirsten Wehnerts Fond, Aage Bangs Fond, The A. P. Møller Foundation for the Advancement of Medical Science (Fonden til Lægevidenskabens Fremme), and the Oda og Hans Svenningsens Fond. L.B.R. is enrolled at the Graduate School of HEALTH, Aarhus University, Aarhus.

Disclosure of potential conflict of interest: J. G. Mikkelsen reports receipt of research funding from CSL Behring and speaking fees from Takeda. The rest of the authors declare that they have no relevant conflicts of interest.

We thank Charlotte Thornild Møller for technical assistance. We acknowledge AU Health Bioimaging Core Facility for use of equipment and imaging facility support. Flow cytometry was performed at the FACS Core Facility, Aarhus University, Aarhus. We thank Anette Bygum for clinical insight and scientific discussions related to this work.

Key message

- **Our novel functional classification of disease-associated *SERPING1* variants suggests that different *SERPING1* gene variants drive the pathogenicity of HAE through different, and in some cases overlapping, molecular disease mechanisms, with a high prevalence of dominant-negative disease mechanisms among the studied variants.**

REFERENCES

1. Bork K, Meng G, Staubach P, Hardt J. Hereditary angioedema: new findings concerning symptoms, affected organs, and course. Am J Med 2006;119:267-74.
2. Zotter Z, Csuka D, Szabó E, Czaller I, Nébenführer Z, Temesszentandrási G, et al. The influence of trigger factors on hereditary angioedema due to C1-inhibitor deficiency. Orphanet J Rare Dis 2014;9:44.
3. Agostoni A, Cicardi M. Hereditary and Acquired C1-inhibitor deficiency: biological and clinical characteristics in 235 patients. Medicine (Baltimore) 1992;71:206-15.
4. Mete Gökmen N, Rodríguez-Alcalde C, Gülbahar O, Lopez-Trascasa M, Onay H, López-Lera A. Novel homozygous variants in the *SERPING1* gene in two Turkish families with hereditary angioedema of recessive inheritance. Immunol Cell Biol 2020;98:693-9.
5. Caccia S, Suffritti C, Carzaniga T, Berardelli R, Berra S, Martorana V, et al. Intermittent C1-inhibitor deficiency associated with recessive inheritance: functional and structural insight. Sci Rep 2018;8:977.
6. Zuraw BL, Christiansen SC. HAE pathophysiology and underlying mechanisms. Clin Rev Allergy Immunol 2016;51:216-29.
7. Germenis AE, Speletas M. Genetics of hereditary angioedema revisited. Clin Rev Allergy Immunol 2016;51:170-82.
8. Rosen FS, Pensky J, Donaldson V, Charache P. Hereditary angioneurotic edema: two genetic variants. Science 1965;148(3672):957-8.
9. Gregorek H, Kokai M, Hidvegi T, Fust G, Sabbouh K, Madalinski K. Concentration of C1 inhibitor in sera of healthy blood donors as studied by immunoenzymatic assay. Complement Inflamm 1991;8:310-2.
10. Kaplan AP, Ghebrehiwet B. The plasma bradykinin-forming pathways and its interrelationships with complement. Mol Immunol 2010;47:2161-9.
11. Nussberger J, Cugno M, Amstutz C, Cicardi M, Pellacani A, Agostoni A. Plasma bradykinin in angio-oedema. Lancet 1998;351(9117):1693-7.
12. Ratnoff OD, Pensky J, Ogston D, Naff GB. The inhibition of plasmin, plasma kallikrein, plasma permeability factor and the C1r subcomponent of the first component of complement by serum C1 esterase inhibitor. J Exp Med 1969;129:315-31.
13. Schreiber AD, Kaplan AP, Austen KF. Inhibition by C1INH of Hagemann factor fragment activation of coagulation, fibrinolysis, and kinin generation. J Clin Invest 1973;52:1402-9.
14. Bouillet L, Mannic T, Arboleas M, Subileau M, Massot C, Drouet C, et al. Hereditary angioedema: key role for kallikrein and bradykinin in vascular endothelial–cadherin cleavage and edema formation. J Allergy Clin Immunol 2011;128:232-4.
15. Orsenigo F, Giampietro C, Ferrari A, Corada M, Galaup A, Sigismund S, et al. Phosphorylation of VE-cadherin is modulated by haemodynamic forces and contributes to the regulation of vascular permeability in vivo. Nat Commun 2012;3:1208.
16. Moncada S, Palmer R, Higgs E. Nitric oxide: physiology, pathophysiology, and pharmacology. Pharmacol Rev 1991;43:109-42.
17. Palmer R, Ashton D, Moncada S. Vascular endothelial cells synthesize nitric oxide from l-arginine. Nature 1988;16(333):664-6.
18. Busse R, Mülsch A. Calcium-dependent nitric oxide synthesis in endothelial cytosol is mediated by calmodulin. FEBS Lett 1990;265:133-6.
19. Archer SL, Huang JM, Hampl V, Nelson DP, Shultz PJ, Weir EK. Nitric oxide and cGMP cause vasorelaxation by activation of a charybdotoxin-sensitive K channel by cGMP-dependent protein kinase. Proc Natl Acad Sci U S A 1994;91:7583-7.
20. Fox RH, Goldsmith R, Kidd DJ, Lewis GP. Bradykinin as a vasodilator in man. J Physiol 1961;157:539-58.
21. Walford HH, Zuraw BL. Current update on cellular and molecular mechanisms of hereditary angioedema. Ann Allergy Asthma Immunol 2014;112:413-8.
22. Kaplan A. Enzymatic pathways in the pathogenesis of hereditary angioedema: the role of C1 inhibitor therapy. J Allergy Clin Immunol 2010;126:918-25.
23. Cicardi M, Igarashi T. Molecular basis for the deficiency of complement 1 inhibitor in type I hereditary angioneurotic edema. J Clin Invest 1987;79:698-702.
24. Davis AE. C1 inhibitor and hereditary angioneurotic edema. Annu Rev 1988;6:595-628.
25. Rosen FS, Alper CA, Pensky J, Klemperer MR, Donaldson VH. Genetically determined heterogeneity of the C1 esterase inhibitor in patients with hereditary angioneurotic edema. J Clin Invest 1971;50:2143-9.
26. Hack CE, Relan A, Van Amersfoort ES, Cicardi M. Target levels of functional C1-inhibitor in hereditary angioedema. Allergy 2012;67:123-30.
27. Ernst SC, Circolo A, Davis AE 3rd, Gheesling-Mullis K, Fliesler M, Strunk RC. Impaired production of both normal and mutant C1 inhibitor proteins in type I hereditary angioedema with a duplication in exon 8. J Immunol 1996;157:405-10.
28. Kramer J, Rosen F, Colten H. Transinhibition of C1 inhibitor synthesis in type I hereditary angioneurotic edema. J Clin Invest 1993;91:1258-62.
29. Verpy E, Couture-Tosi E, Eldering E, Lopez-Trascasa M, Späth P, Meo T, et al. Crucial residues in the carboxy-terminal end of C1 inhibitor revealed by pathogenic mutants impaired in secretion or function. J Clin Invest 1995;95:350-9.
30. Woo P, Lachmann PJL, Harrison RA, Amos N, Cooper C, Rosen FS. Simultaneous turnover of normal and dysfunctional C1 inhibitor as a probe of *in vivo* activation of C1 and contact activatable proteases. Clin Exp Immunol 1985;61:1-8.
31. Ponard D, Gaboriaud C, Charignon D, Ghannam A, Wagenaar-Bos IGA, Roem D, et al. *SERPING1* mutation update: mutation spectrum and C1 inhibitor phenotypes. Hum Mutat 2020;41:38-57.
32. Huntington JA. Serpin structure, function and dysfunction. J Thromb Haemost 2011;9(1 suppl):26-34.
33. Gettins PGW. Serpin structure, mechanism, and function. Chem Rev 2002;102:4751-803.
34. Wei A, Rubin H, Copperman BS, Christianson DW. Crystal structure of an uncleaved serpin reveals the conformation of an inhibitory reactive loop. Nat Struct Biol 1994;1:251-8.

35. Bruch M, Weiss V, Engel J. Plasma serine proteinase inhibitors (serpins) exhibit major conformational changes and a large increase in conformational stability upon cleavage at their reactive sites. J Biol Chem 1988;263:16626-30.
36. Egelund R, Rodenburg KW, Andreasen PA, Rasmussen MS, Guldberg RE, Petersen TE. An ester bond linking a fragment of a serine proteinase to its serpin inhibitor. Biochemistry 1998;37:6375-9.
37. Huntington JA, Read RJ, Carrell RW. Structure of a serpin–protease complex shows inhibition by deformation. Nature 2000;407(6806):923-6.
38. Schreuder H, Boer B, Dijkema R, Mulders J, Theunissen H, Grootenhuis P, et al. The intact and cleaved human antithrombin III complex as a model for serpin–proteinase interactions. Nat Struct Biol 1994;1:48-54.
39. Khan MS, Singh P, Azhar A, Naseem A, Rashid Q, Kabir MA, et al. Serpin inhibition mechanism: a delicate balance between native metastable state and polymerization. J Amino Acids 2011;2011:10.
40. Chuang YJ, Swanson R, Raja SM, Bock SC, Olson ST. The antithrombin P1 residue is important for target proteinase specificity but not for heparin activation of the serpin. Characterization of P1 antithrombin variants with altered proteinase specificity but normal heparin activation. Biochemistry 2001;40:6670-9.
41. Sulikowski T, Bauer BA, Patston PA. alpha(1)-Proteinase inhibitor mutants with specificity for plasma kallikrein and C1s but not C1. Protein Sci 2002;11:2230-6.
42. Irving JA, Pike RN, Lesk AM, Whisstock JC. Phylogeny of the serpin superfamily: implications of patterns of amino acid conservation for structure and function. Genome Res 2000;10:1845-64.
43. Zhou A, Carrell RW, Huntington JA. The serpin inhibitory mechanism is critically dependent on the length of the reactive center loop. J Biol Chem 2001;276:27541-7.
44. Hopkins PCR, Carrell RW, Stone SR. Effects of mutations in the hinge region of serpins. Biochemistry 1993;32:7650-7.
45. Whisstock JC, Skinner R, Carrell RW, Lesk a M. Conformational changes in serpins: I. The native and cleaved conformations of alpha(1)-antitrypsin. J Mol Biol 2000;296:685-99.
46. Lawrence DA, Ginsburg D, Day DE, Berkenpas MB, Verhamme IM, Kvassman J, et al. Serpin–protease complexes are trapped as stable acyl-enzyme intermediates. J Biol Chem 1995;270:25309-12.
47. Maddur AA, Swanson R, Izaguirre G, Gettins PGW, Olson ST. Kinetic intermediates en route to the final serpin-protease. J Biol Chem 2013;288:32020-35.
48. Haslund D, Nejsum LN, Giehm J, Invest JC, Haslund D, Ryø LB, et al. Dominant-negative *SERPING1* variants cause intracellular retention of C1 inhibitor in hereditary angioedema. J Clin Invest 2019;129:388-405.
49. Yasuno S, Ansai O, Hayashi R, Nakamura S, Shimomura Y. Evidence for a dominant-negative effect of a missense mutation in the *SERPING1* gene responsible for hereditary angioedema type I. J Dermatol 2021;48:1243-9.
50. Ren Z, Zhao S, Li T, Wedner HJ, Atkinson JP. Insights into the pathogenesis of hereditary angioedema employing genetic sequencing and recombinant protein expression analyses. J Allergy Clin Immunol 2023;151:1040-9.e5.
51. Madsen DE, Hansen S, Gram J, Bygum A, Drouet C, Sidelmann JJ. Presence of C1-inhibitor polymers in a subset of patients suffering from hereditary angioedema. PLoS One 2014;9:1-7.
52. Madsen DE, Sidelmann JJ, Biltoft D, Gram J, Hansen S. C1-inhibitor polymers activate the FXII-dependent kallikrein–kinin system: implication for a role in hereditary angioedema. Biochim Biophys Acta 2015;1850:1336-42.
53. Laimer M, Klausegger A, Aberer W, Oender K, Steinhuber M, Lanschuetzer CM, et al. Haploinsufficiency due to deletion within the 3′-UTR of C1-INH-gene associated with hereditary angioedema. Genet Med 2006;8:249-54.
54. Colobran R, Pujol-Borrell R, Hernandez-Gonzalez M, Guilarte M. A novel splice site mutation in the *SERPING1* gene leads to haploinsufficiency by complete degradation of the mutant allele mRNA in a case of familial hereditary angioedema. J Clin Immunol 2014;34:521-3.
55. Quastel M, Harrison R, Cicardi M, Alper CA, Rosen FS. Behavior *in vivo* of normal and dysfunctional C1 inhibitor in normal subjects and patients with hereditary angioneurotic edema. J Clin Invest 1983;71:1041-6.
56. Marques PI, Ferreira Z, Martins M, Figueiredo J, Silva DI, Castro P, et al. *SERPINA2* is a novel gene with a divergent function from *SERPINA1*. PLoS One 2013;8:e66889.
57. Pihl R, Jensen RK, Poulsen EC, Jensen L, Hansen AG, Thøgersen IB, et al. ITIH4 acts as a protease inhibitor by a novel inhibitory mechanism. Sci Adv 2021;7:eaba7381.
58. Kajdácsi E, Jandrasics Z, Veszeli N, Makó V, Koncz A, Gulyás D, et al. Patterns of C1-inhibitor/plasma serine protease complexes in healthy humans and in hereditary angioedema patients. Front Immunol 2020;11:794.
59. Troldborg A, Hansen A, Hansen SWK, Jensenius JC, Stengaard-Pedersen K, Thiel S. Lectin complement pathway proteins in healthy individuals. Clin Exp Immunol 2017;188:138-47.
60. An JK, Blomenkamp K, Lindblad D, Teckman JH. Quantitative isolation of α_1AT mutant Z protein polymers from human and mouse livers and the effect of heat. Hepatology 2005;41:160-7.
61. Shen S, Sanchez ME, Blomenkamp K, Corcoran EM, Marco E, Yudkoff CJ, et al. Amelioration of alpha-1 antitrypsin deficiency diseases with genome editing in transgenic mice. Hum Gene Ther 2018;29:861-73.
62. de Maat S, Björkqvist J, Suffritti C, Wiesenekker CP, Nagtegaal W, Koekman A, et al. Plasmin is a natural trigger for bradykinin production in patients with hereditary angioedema with factor XII mutations. J Allergy Clin Immunol 2016;138:1414-23.e9.
63. Bos IGA, Lubbers YTP, Roem D, Abrahams JP, Hack CE, Eldering E. The functional integrity of the serpin domain of C1-inhibitor depends on the unique N-terminal domain, as revealed by a pathological mutant. J Biol Chem 2003;278:29463-70.
64. Lomas DA, Evans DL, Finch JT, Carrell RW. The mechanism of Z alpha 1–antitrypsin accumulation in the liver. Nature 1992;357:605-7.
65. Lomas DA, Mahadeva R, Lomas DA, Mahadeva R. α_1-Antitrypsin polymerization and the serpinopathies: pathobiology and prospects for therapy. J Clin Invest 2002;110:1585-90.
66. Davis RL, Shrimpton AE, Holohan PD, Bradshaw C, Feiglin D, Collins GH, et al. Familial dementia caused by polymerization of mutant neuroserpin. Nature 1999;401(6751):376-9.
67. Yazaki M, Liepnieks JJ, Murrell JR, Takao M, Guenther B, Piccardo P, et al. Biochemical characterization of a neuroserpin variant associated with hereditary dementia. Am J Pathol 2001;158:227-33.
68. Mahadeva R, Chang WS, Dafforn TR, Oakley DJ, Foreman RC, Calvin J, et al. Heteropolymerization of S, I, and Z alpha$_1$-antitrypsin and liver cirrhosis. J Clin Invest 1999;103:999-1006.
69. Mete Gökmen N, Gülbahar O, Onay H, Peker Koc Z, Özgül S, Köse T, et al. Deletions in *SERPING1* lead to lower C1 inhibitor function: lower C1 inhibitor function can predict disease severity. Int Arch Allergy Immunol 2019;178:50-9.
70. Guryanova I, Suffritti C, Parolin D, Zanichelli A, Ishchanka N, Polyakova E, et al. Hereditary angioedema due to C1 inhibitor deficiency in Belarus: epidemiology, access to diagnosis and seven novel mutations in *SERPING1* gene. Clin Mol Allergy 2021;19:1-8.
71. Ronzoni R, Ferrarotti I, D'acunto E, Balderacchi AM, Ottaviani S, Lomas DA, et al. The importance of n186 in the alpha-1–antitrypsin shutter region is revealed by the novel bologna deficiency variant. Int J Mol Sci 2021;22:1-18.
72. Ingwersen T, Linnenberg C, D'Acunto E, Temori S, Paolucci I, Wasilewski D, et al. G392E neuroserpin causing the dementia FENIB is secreted from cells but is not synaptotoxic. Sci Rep 2021;11:1-13.
73. Fra A, Cosmi F, Ordoñez A, Berardelli R, Perez J, Guadagno NA, et al. Polymers of Z α_1-antitrypsin are secreted in cell models of disease. Eur Respir J 2016;47:1005-9.
74. Speletas M, Szilágyi, Csuka D, Koutsostathis N, Psarros F, Moldovan D, et al. F12-46C/T polymorphism as modifier of the clinical phenotype of hereditary angioedema. Allergy 2015;70:1661-4.
75. Veronez CL, Aabom A, Martin RP, Filippelli-Silva R, Gonçalves RF, Nicolicht P, et al. Genetic variation of kallikrein–kinin system and related genes in patients with hereditary angioedema. Front Med 2019;6:1-6.
76. Brackertz D, Isler E, Kueppers F. Half-life of CINH in hereditary angioneurotic oedema (HAE). Clin Exp Allergy 1975;5:89-94.
77. Pappalardo E, Caccia S, Suffritti C, Tordai A, Zingale LC, Cicardi M. Mutation screening of C1 inhibitor gene in 108 unrelated families with hereditary angioedema: functional and structural correlates. Mol Immunol 2008;45:3536-44.
78. Martinho A, Mendes J, Simões O, Nunes R, Gomes J, Castro ED, et al. Mutations analysis of C1 inhibitor coding sequence gene among Portuguese patients with hereditary angioedema. Mol Immunol 2013;53:431-4.
79. Roche O, Blanch A, Duponchel C, Fontán G, Tosi M, López-Trascasa M. Hereditary angioedema: the mutation spectrum of *SERPING1*/C1NH in a large Spanish cohort. Hum Mutat 2005;26:135-44.
80. Cagini N, Lopes Veronez C, Navickas Constantino-Silva R, Buzolin M, Martin RP, Sevciovic Grumach A, et al. New mutations in *SERPING1* gene of Brazilian patients with hereditary angioedema. Biol Chem 2016;397:337-44.
81. Bafunno V, Bova M, Loffredo S, Divella C, Petraroli A, Marone G, et al. Mutational spectrum of the C1 inhibitor gene in a cohort of italian patients with hereditary angioedema: description of nine novel mutations. Ann Hum Genet 2014;78:73-82.
82. Grivčeva-Panovska V, Košnik M, Korošec P, Andrejević S, Karadža-Lapić L, Rijavec M. Hereditary angioedema due to C1-inhibitor deficiency in Macedonia: clinical characteristics, novel *SERPING1* mutations and genetic factors modifying the clinical phenotype. Ann Med 2018;50:269-76.
83. Zuraw BL, Herschbach J. Detection of C1 inhibitor mutations in patients with hereditary angioedema. J Allergy Clin Immunol 2000;105:541-6.

84. Pappalardo E, Cicardi M, Duponchel C, Carugati A, Choquet S, Agostoni A, et al. Frequent *de novo* mutations and exon deletions in the C1 inhibitor gene of patients with angioedema. J Allergy Clin Immunol 2000;106: 1147-54.

85. Verpy E, Biasotto M, Brai M, Misiano G, Meo T, Tosi M. Exhaustive mutation scanning by fluorescence-assisted mismatch analysis discloses new genotype–phenotype correlations in angioedema. Am J Hum Genet 1996;59: 308-19.

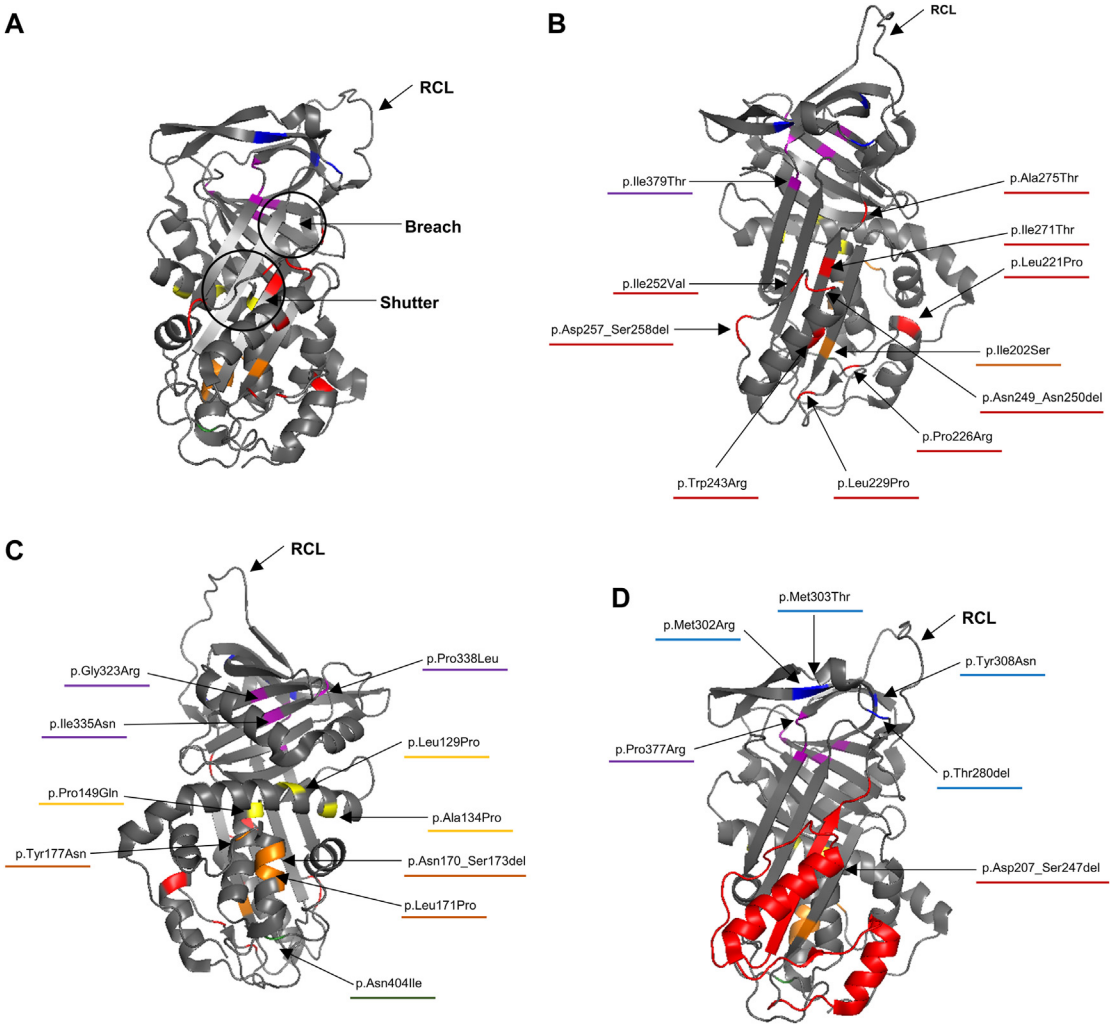

FIG E1. C1INH protein structure. **(A)** Structure of C1INH (protein data bank entry 5DU3). *Black arrows* indicate location of RCL, shutter, and breach regions. **(B-D)** Structure of C1INH from different perspectives to illustrate locations of amino acid changes found in C1INH encoded by studied *SERPING1* variants. Colors indicate exon of *SERPING1* gene (Fig 1, *A*) on which variant is located: *yellow,* exon 3; *orange,* exon 4; *red,* exon 5; *blue,* exon 6; *purple,* exon 7; and *green,* exon 8. SERPING1[c.161T>A] is not included because it is located at the N-terminal nonserpin domain, which is not depicted in the tertiary C1INH protein structure. Figure created by PyMol.

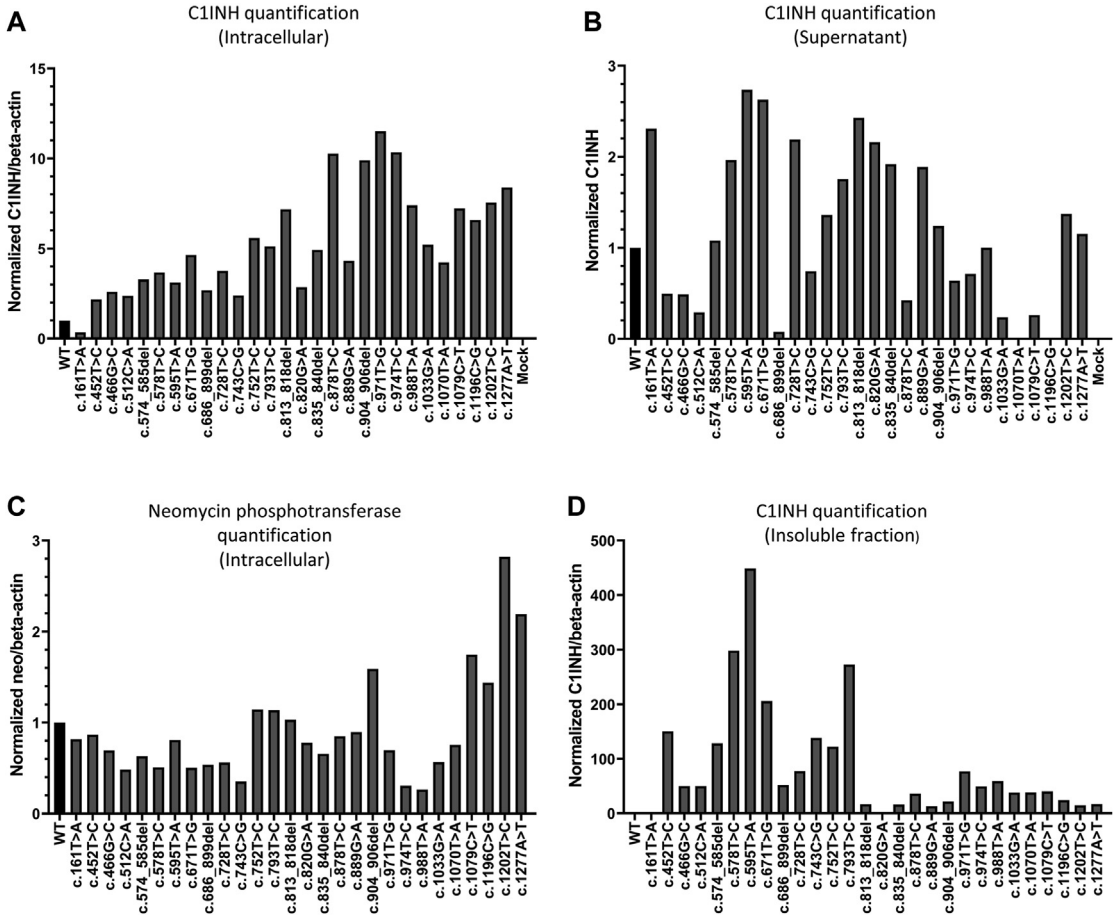

FIG E2. Western blot quantifications. **(A)** Quantification of signal intensity of C1INH[variant] detected intracellularly after single transfections normalized to β-actin. **(B)** Quantification of signal intensity of C1INH[variant] detected in supernatant after single transfections. Normalized to intensity of WT band. **(C)** Quantification of signal intensity of neomycin phosphotransferase detected intracellularly after single transfections normalized to β-actin. **(D)** Quantification of signal intensity of C1INH[variant] detected in insoluble fraction after single transfections normalized to β-actin.

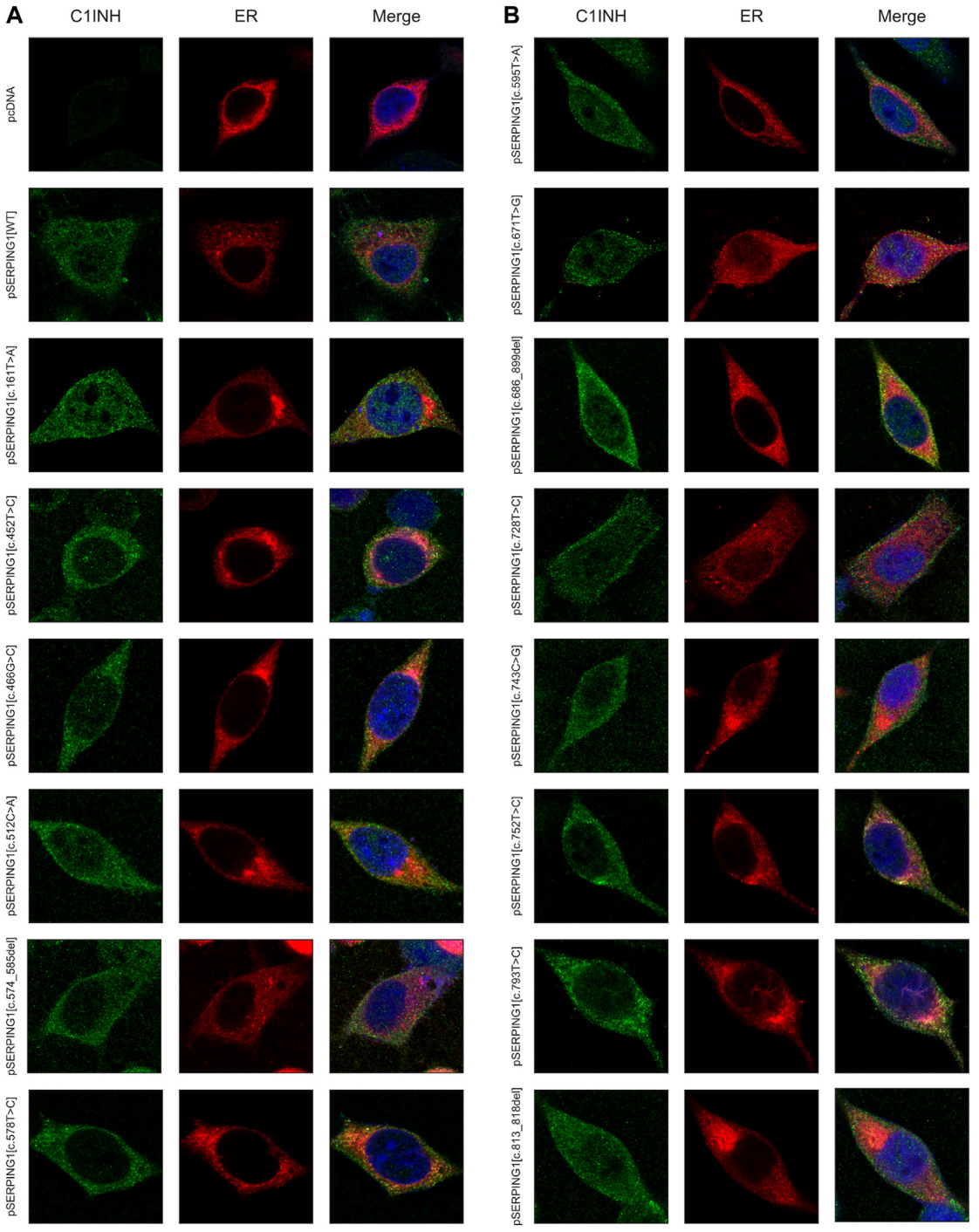

FIG E3. C1INH encoded by studied *SERPING1* variants colocalize with ER. Confocal microscopy of HeLa cells transfected with 900 ng pSERPING1[variant] and 200 ng of expression plasmid encoding Tomato-Calreticulin to visualize ER *(red).* At 72 hours after transfection, cells were fixed. C1INH protein was visualized by anti-C1INH antibody *(green),* and cell nuclei were visualized with Hoechst *(blue).* Scale bars: 5 μm. Representative images are shown.

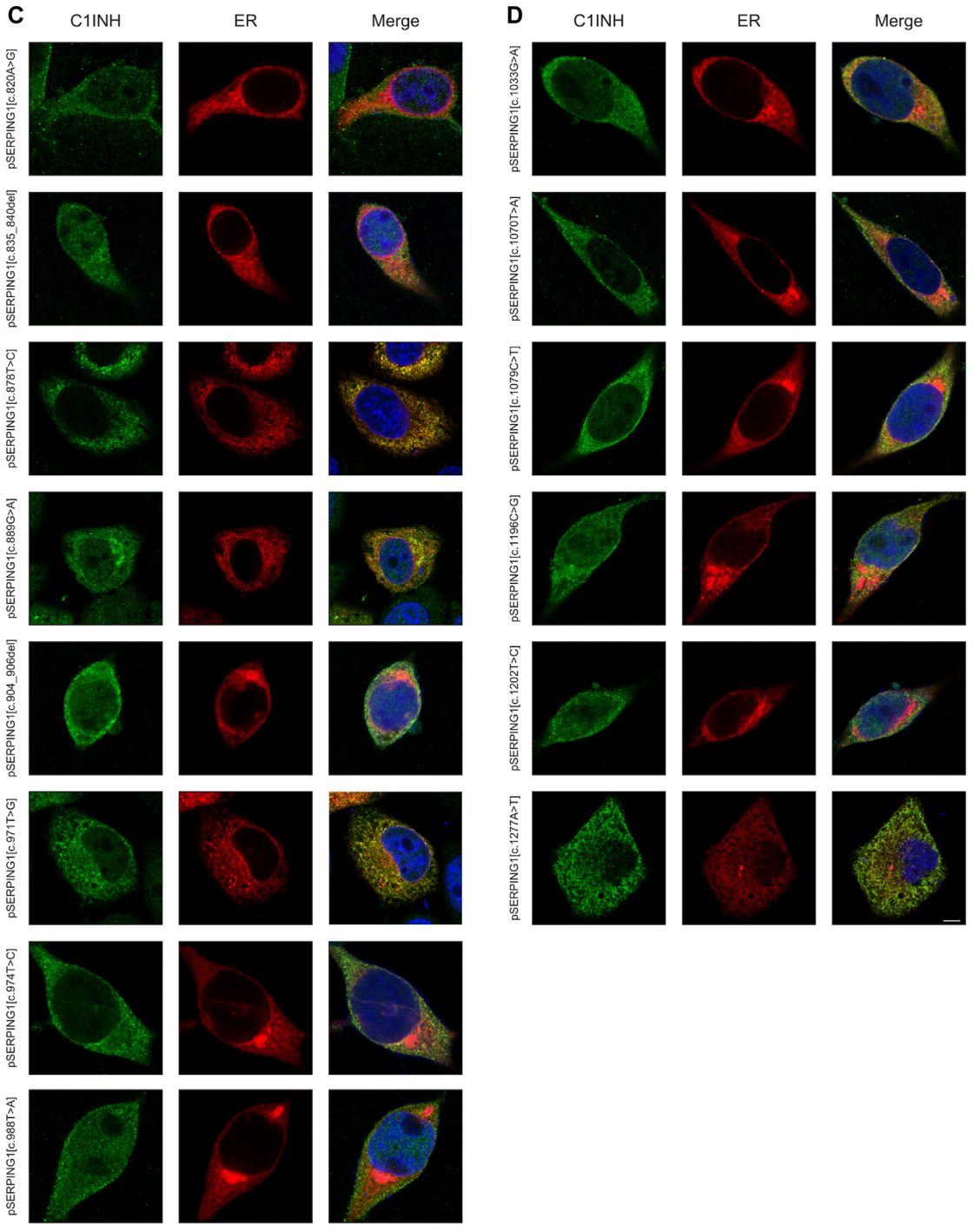

FIG E3. *(Continued).*

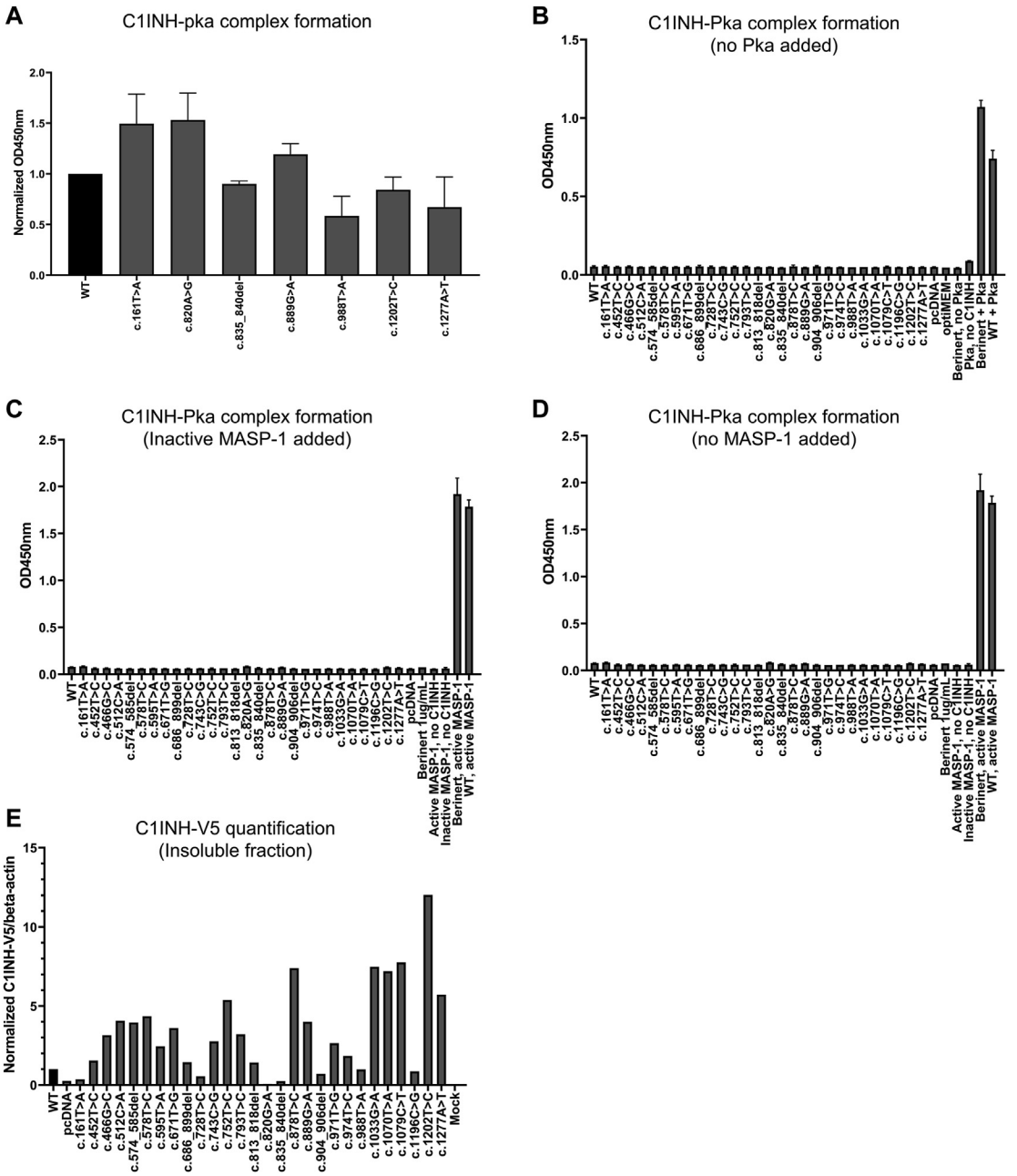

FIG E4. **(A)** C1INH-pKa complex ELISA for samples reaching high OD values diluted further. **(B)** C1INH-pKa complex formation using C1INH samples with no prior incubation with pKa. **(C)** C1INH–MASP-1 complex formation using C1INH samples incubated with inactive MASP-1. **(D)** C1INH–MASP-1 complex using C1INH samples with no prior incubation with MASP-1. **(E)** Quantification of Western blot signal intensity of normal C1INH-V5 detected in insoluble fraction after cotransfection of pSERPING1[WT]-V5 and pSERPING1[variant]. *OD,* Optical density.

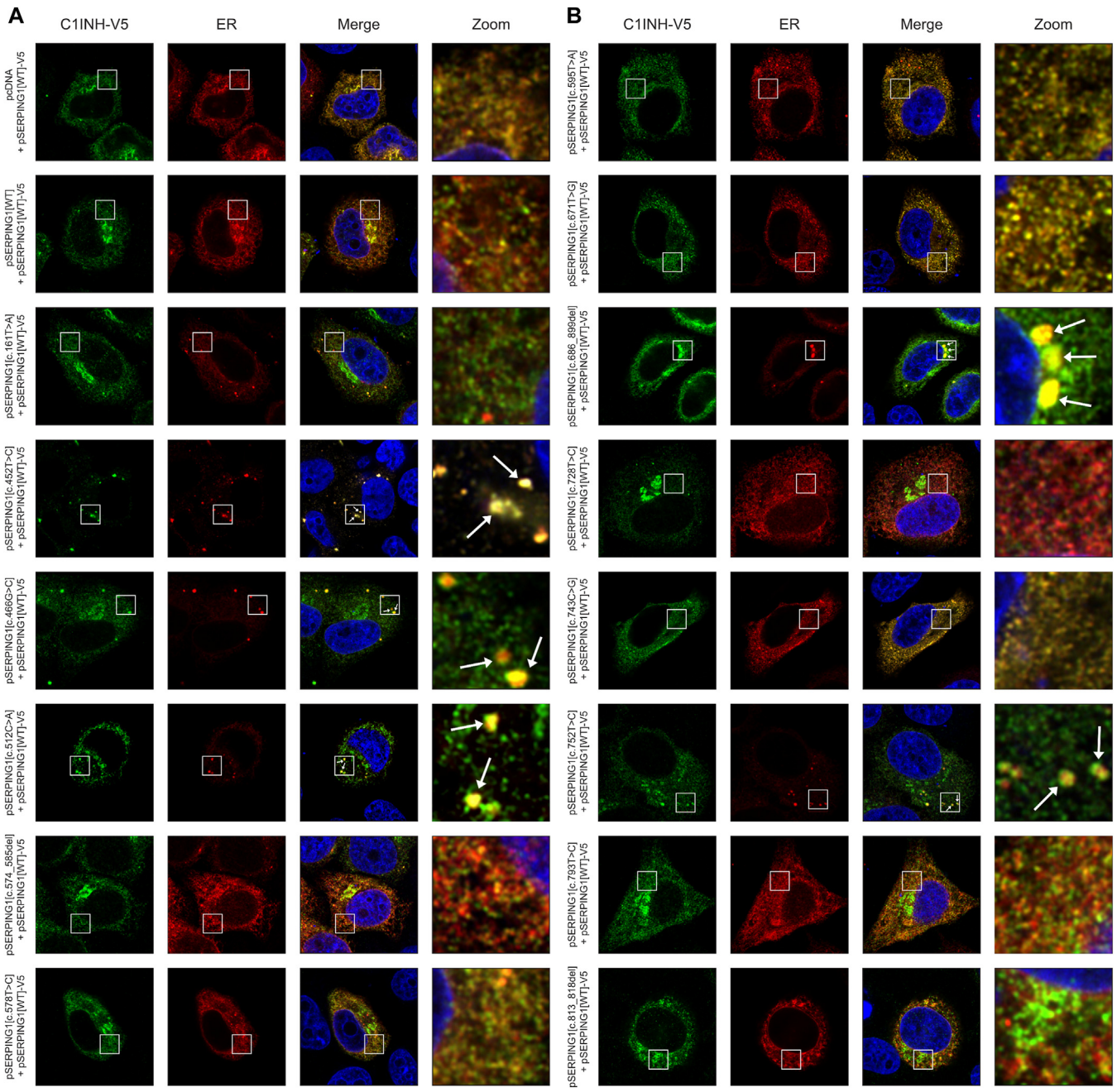

FIG E5. Coexpression of normal and mutated C1INH induces formation of intracellular C1INH foci colocalizing with ER. HeLa cells were cotransfected with 450 ng pSERPING1[WT]-V5, 450 ng pSERPING1 [variant], and 200 ng of expression plasmid encoding Tomato-Calreticulin to visualize ER. At 72 hours after transfection, cells were fixed, and normal V5-tagged C1INH was visualized with anti-V5 antibody *(green).* Cell nuclei were visualized with DAPI *(blue).* Examples of focus formation are indicated by *white arrows.* Scale bars: 5 μm. Representative images are shown. *DAPI,* 4′,6-Diamidino-2-phenylindole.

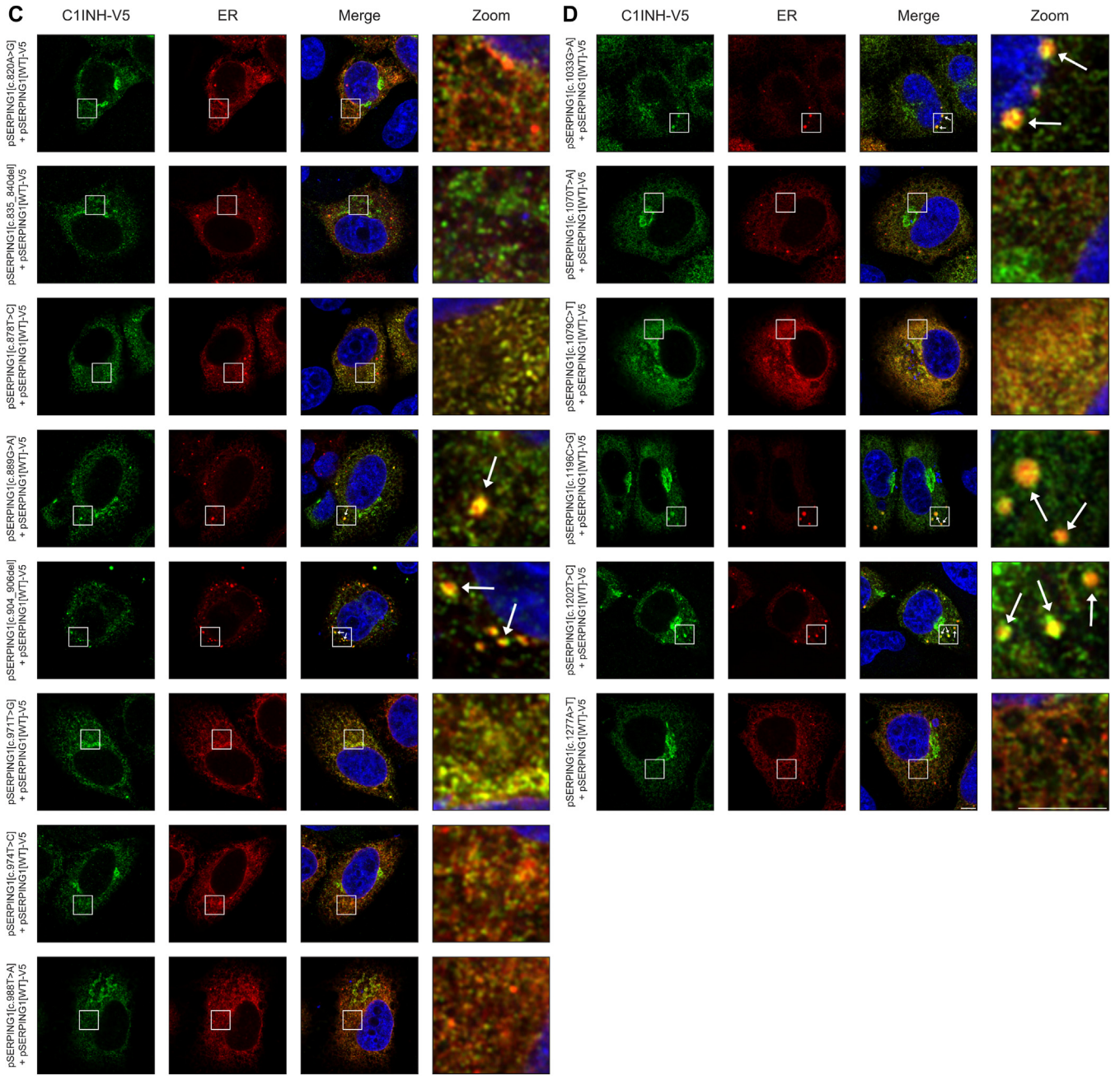

FIG E5. *(Continued).*

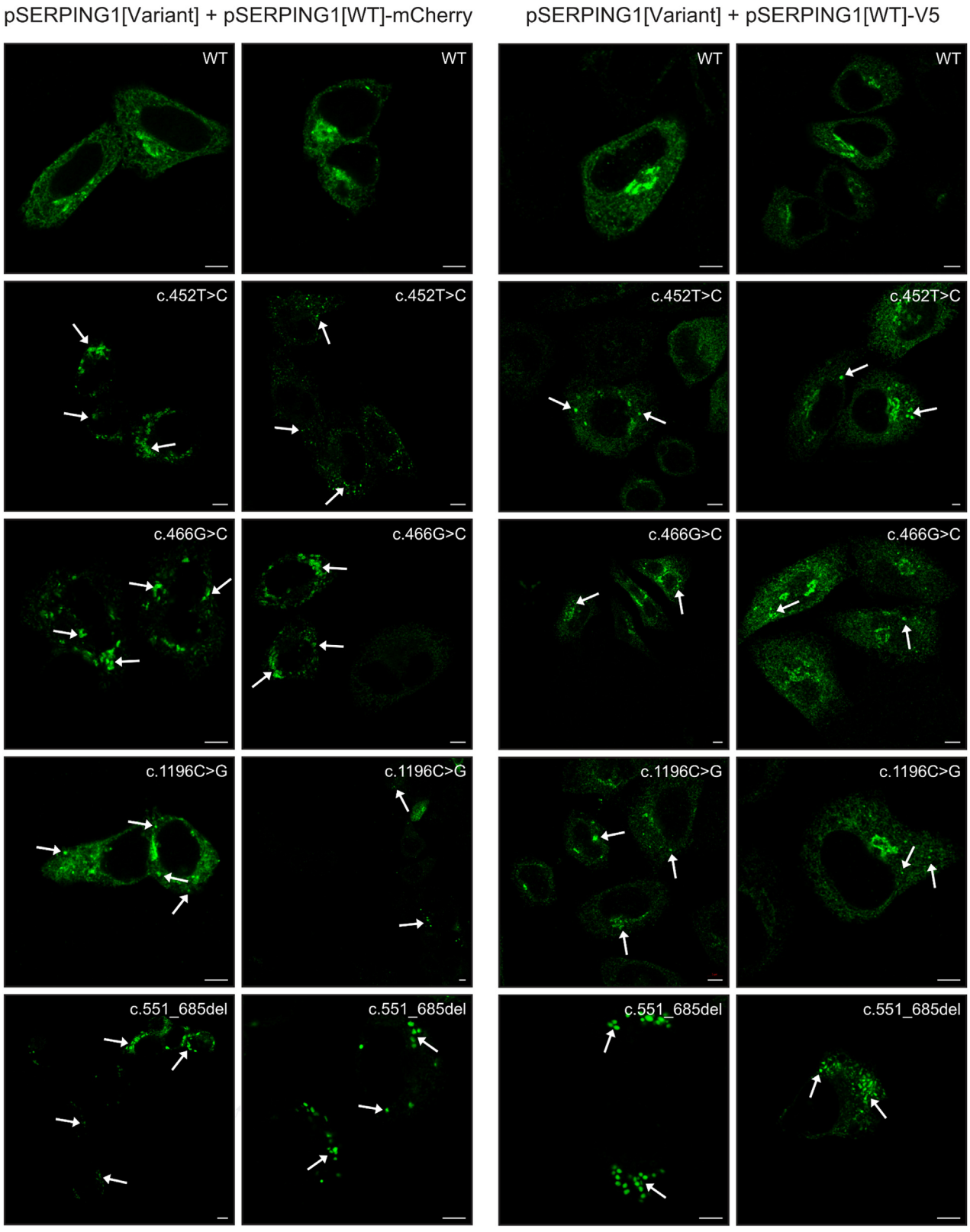

FIG E6. Formation of intracellular C1INH foci with both mCherry- and V5-tagged C1INH. HeLa cells were cotransfected with 450 ng pSERPING1[variant] and 450 ng of either pSERPING1[WT]-mCherry or pSERPING1[WT]-V5. At 72 hours after transfection, cells were fixed, and normal-tagged C1INH was visualized *(green).* For visualization of V5-tagged C1INH, anti-V5 antibody *(green)* was used. Examples of focus formation are indicated by *white arrows.* SERPING1 variant c.551_686del, which we have previously shown to induce formation of C1INH aggregates, was included as positive control. Scale bars: 5 μm. Representative images are shown.

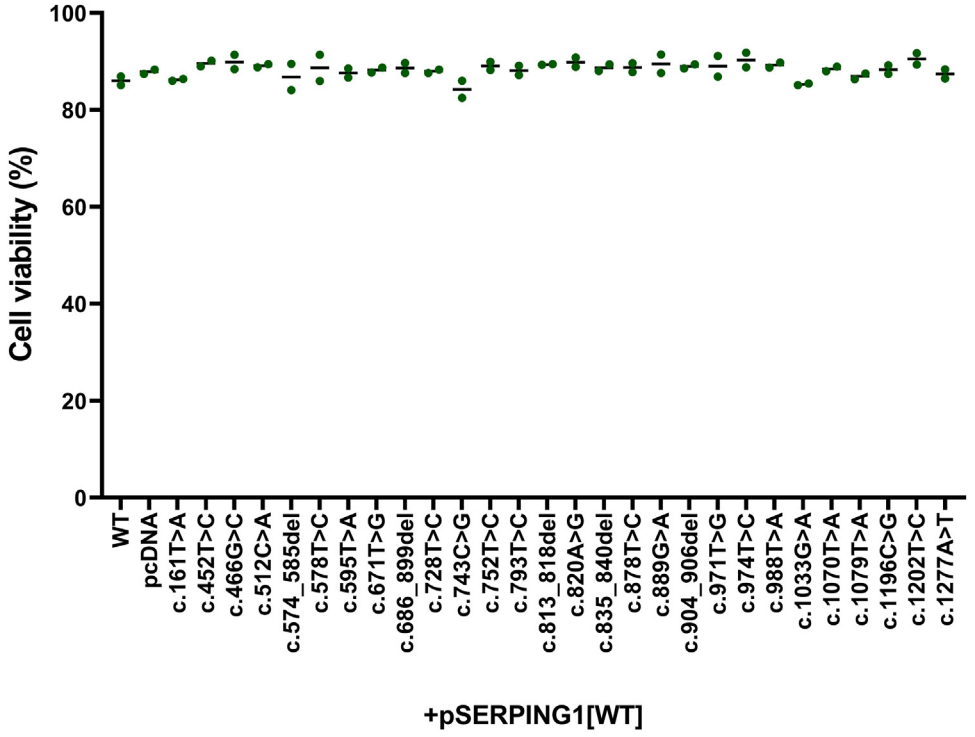

FIG E7. Coexpression of normal and mutated C1INH does not affect cell viability. HeLa cells were cotransfected with 450 ng pSERPING1[WT] and 450 ng pSERPING1[variant]. At 72 hours after transfection, cells were collected for flow cytometry. Cell viability was determined by PI staining. *Lines* represent mean of 2 independent transfections, with *dots* corresponding to mean of each transfection measured in technical duplicates. *PI,* Propidium iodide.